Physics – Uspekhi **62** (4) 340 – 353 (2019)

REVIEWS OF TOPICAL PROBLEMS PACS numbers: 12.20.Ds, **32.80. – t**

High-energy electroproduction in an atomic field

P A Krachkov, A I Milstein

DOI: https://doi.org/10.3367/UFNe.2018.03.038425

Contents

Abstract. We discuss the most recent results in studies of high-energy electroproduction in an atomic field. Production of an e^+e^- pair by a relativistic electron, relativistic muon, or light nucleus and production of a $\mu^+\mu^-$ pair by a relativistic electron are reviewed. We focus on an accurate account of the interaction of the incoming particle and produced pair with the atomic field (Coulomb corrections). In all the considered cases, interaction of the particle that produces a virtual photon with the atomic field is shown to significantly change the differential cross section of the process (differential with respect to the momentum of the photon-emitting particle), in disagreement with the generally accepted opinion. However, the process cross section integrated over that momentum is only weakly affected by the interaction. Pair production in an unbound or bound state (positronium, muonium, and dimuonium) is discussed.

Keywords: electroproduction, positronium, muonium, dimuonium, strong atomic field

1. Introduction

Processes of e^+e^- and $\mu^+\mu^-$ pair production in collisions of charged particles with atoms (electroproduction) are fundamental processes of quantum electrodynamics. Exact knowledge of their cross sections is of utmost importance for the description of interactions between charged particles and matter. This is why theoretical studies of electroproduction began as early as the 1930s; a large number of papers have been published since then. Differential cross sections and various integral characteristics of electroproduction of electron–positron pairs by an ultrarelativistic electron in an atomic field are studied in Refs [1–9] in the lowest order of the perturbation theory in the parameter $\eta = Z\alpha$ (the Born approximation), where Z is the atom charge number, α is the fine structure constant, and $\hbar = c = 1$. Many papers are devoted to the electroproduction of e^+e^- pairs by a heavy particle (muon or nucleus) in an atomic field [10–16] and $\mu^+\mu^-$ pairs by a relativistic electron in an atomic field [1, 2, 17].

A pair of produced particles can be either in the unbound or in a bound (positronium, dimuonium) state. Properties of dimuonium have been discussed in numerous papers [18–30]. Because this hydrogen-like atom is 200 times smaller than positronium, it is promising for the search for new physics. The production of dimuonium has not been discovered thus far, but there are several suggestions as to how to find it. An experimental setup based on the production of dimuonium in e^+e^- annihilation [31] is being developed at the Budker Institute of Nuclear Physics, Siberian Branch, Russian Academy of Sciences. At the Jefferson Laboratory (USA), it is planned to produce dimuonium through the interaction of electrons with a tungsten target [32]. At the Fermi National Laboratory (USA), it is proposed to find dimuonium in $\eta \to \gamma(\mu^+\mu^-)$ decays, where the η meson is created in the interaction of protons with a beryllium target [33]. An experiment is also discussed on dimuonium production using a low-energy muon beam [34].

The question arises as to whether anything qualitatively new and interesting can still be found given such a long history of studying electroproduction? The answer to this question turns out to be positive: in electroproduction on heavy atoms, the parameter $\eta = Z\alpha$ is not small and we have to go beyond the perturbation theory in this parameter, i.e., find Coulomb corrections. The Coulomb corrections can be related to interactions of the particles of the produced pair, as well as the particle emitting a virtual photon, with the atomic field. All the Coulomb corrections discussed thus far have been related to the process of virtual photon conversion into a

P A Krachkov, A I Milstein Budker Institute of Nuclear Physics, Siberian Branch of the Russian Academy of Sciences, prosp. Akademika Lavrent'eva 11, 630090 Novosibirsk, Russian Federation
E-mail: P.A.Krachkov@inp.nsk.su, A.I.Milstein@inp.nsk.su

Received 29 January 2018
Uspekhi Fizicheskikh Nauk **189** (4) 359 – 373 (2019)
DOI: https://doi.org/10.3367/UFNr.2018.03.038425
Translated by S D Danilov; edited by A M Semikhatov

pair, whereas corrections related to the virtual photon emission have been completely ignored. It was simply assumed that they do not influence the process cross section. The incoming particle was considered to be either a source of equivalent photons or the source of an external field for motion along a straight trajectory with a fixed impact parameter; alternatively, the wave function of the incoming particle was modeled as a plane wave. Solving the problem with the interaction of both particles in the produced pair and the particle emitting a virtual photon with the atomic field taken into account exactly was technically extremely difficult.

This situation changed with the development of the method of semiclassical Green's functions, enabling a qualitative leap in accurately describing quantum electrodynamic processes in strong electromagnetic fields at high energies. A detailed description of the semiclassical method and a review of numerous latest results obtained with that method can be found in Ref. [35].

The essence of the semiclassical method consists in accounting for contributions from large angular momenta $l \sim p\rho$ of particles involved in the process, where ρ is the characteristic impact parameter and p the particle momentum. The impact parameter can be estimated from the uncertainty relation as $\rho \sim 1/p_\perp$, where $p_\perp \sim p\theta$ and θ is the scattering angle. Hence, for $\theta \ll 1$, we have $l \sim 1/\theta \gg 1$. As a consequence, the expansion in $1/l$ used in the semiclassical approximation is in fact the expansion in small angles between the momenta of the initial and final particles. Just this range contributes most essentially to cross sections of processes in external fields at high energies. The relative accuracy of results for differential cross sections obtained in the semiclassical framework can be estimated by the maximum angle between the momenta of the final particles and the momentum of the initial particle. The accuracy is also governed by the expansion in $1/\gamma_i = m_i/\varepsilon_i \ll 1$, where m_i and ε_i are the energy and mass of the ith particle. The interaction with an external field is treated exactly in the field parameters (the parameter η in our case). In addition, the semiclassical method allows treating the deviation of the atomic field from the Coulomb one at short distances (the effect of a finite nucleus size) and at long distances (screening of the nucleus field by atom electrons).

Relying on the semiclassical method, the processes of e^+e^- pair production by a relativistic electron [36, 37] and a relativistic muon or light nucleus [38], and also the production of a $\mu^+\mu^-$ pair by a relativistic electron [39] can be described exactly in the atomic field parameters. It turned out that in all cases the Coulomb corrections to differential cross sections substantially modify the results obtained in the Born approximation. This concerns corrections related to virtual photon emission and to interactions between the particles of the produced pair and the atomic field. However, the Coulomb corrections related to virtual photon emission do not change the cross section integrated over the final momentum angles of the particle emitting a virtual photon. Our aim in this review is to discuss all these and some other questions related to the electroproduction process.

2. Amplitude of the electroproduction process

In this section, we consider the basic structure of the electroproduction amplitude. Let a charged particle with a mass m_1, initial momentum $\mathbf{p}_1$, and final momentum $\mathbf{p}_2$ create a particle and its antiparticle with masses m_2 and momenta $\mathbf{p}_3$ and $\mathbf{p}_4$ in an atomic field. Figure 1 shows the Feynman diagram that corresponds to the process amplitude. The electroproduction amplitude T can be written as

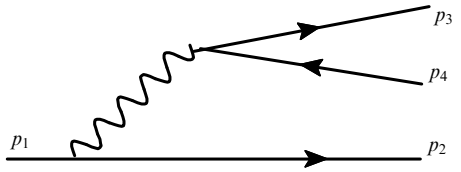

Figure 1. Feynman diagram for the electroproduction amplitude T. The wave line denotes the photon propagator; solid lines correspond to wave functions of charged particles in an atomic field.

$$
\begin{aligned}
T &= \sum_{a,b=1}^{3} \int \frac{\mathrm{d}\mathbf{k}}{(2\pi)^3}\, \mathcal{D}^{ab} j^a J^b\,,\\
\mathcal{D}^{ab} &= -\frac{4\pi}{\omega^2 - k^2 + \mathrm{i}0}\left(\delta^{ab} - \frac{k^a k^b}{\omega^2}\right),\\
\mathbf{j} &= \int \mathrm{d}\mathbf{r} \exp\left(-\mathrm{i}\mathbf{k}\mathbf{r}\right) \bar{u}^-_{\mathbf{p}_2}(\mathbf{r})\boldsymbol{\gamma}\, u^+_{\mathbf{p}_1}(\mathbf{r})\,,\\
\mathbf{J} &= \int \mathrm{d}\mathbf{r} \exp\left(\mathrm{i}\mathbf{k}\mathbf{r}\right) \bar{u}^-_{\mathbf{p}_3}(\mathbf{r})\boldsymbol{\gamma}\, v^+_{\mathbf{p}_4}(\mathbf{r})\,,
\end{aligned}
\tag{1}
$$

where $\omega = \varepsilon_1 - \varepsilon_2 = \varepsilon_3 + \varepsilon_4$, $\varepsilon_i = \sqrt{p_i^2 + m_i^2}$ is the energy of the ith particle, $\mathcal{D}^{\mu\nu}$ is the photon propagator ($\mathcal{D}^{\mu 0} = 0$), γ^ν are the Dirac matrices, $u^+_{\mathbf{p}}(\mathbf{r})$ and $u^-_{\mathbf{p}}(\mathbf{r})$ are the positive-frequency solutions of the Dirac equation in the atomic potential $V(r)$, $v^+_{\mathbf{p}}(\mathbf{r})$ is the negative-frequency solution of the Dirac equation in this potential, and the minus (plus) superscript implies that the asymptotic form of the wave function at long distances contains a spherically converging (diverging) wave in addition to the plane one. The function $\mathbf{j}$ corresponds to the amplitude of virtual photon emission with the momentum $\mathbf{k}$, and the function $\mathbf{J}$ corresponds to the amplitude of particle–antiparticle production by this photon. The functions $\mathbf{j}$ and $\mathbf{J}$ are calculated in the same way as for the bremsstrahlung amplitude of a real photon [41, 42] and the amplitudes of particle and antiparticle production by a real photon in an atomic field [43].

It is convenient to represent the propagator $\mathcal{D}^{ab}$ as

$$
\begin{aligned}
\mathcal{D}^{ab} &= \mathcal{D}^{ab}_\perp + \mathcal{D}^{ab}_\parallel\,,\\
\mathcal{D}^{ab}_\perp &= -\frac{4\pi}{\omega^2 - k^2 + \mathrm{i}0}\left(\delta^{ab} - \frac{k^a k^b}{k^2}\right)\\
&= -\frac{4\pi}{\omega^2 - k^2 + \mathrm{i}0}\sum_{\lambda=\pm} s^{a*}_\lambda s^b_\lambda\,,\\
\mathcal{D}^{ab}_\parallel &= -\frac{4\pi}{\omega^2 k^2}\, k^a k^b\,, \qquad \mathbf{s}_\lambda = \frac{1}{\sqrt{2}}\left(\mathbf{s}_1 + \mathrm{i}\lambda \mathbf{s}_2\right),
\end{aligned}
\tag{2}
$$

where $\mathbf{s_1}$ and $\mathbf{s_2}$ are the unit vectors perpendicular to the vector $\mathbf{k}$. Inserting this expression into Eqn (1), we find

$$
\begin{aligned}
T &= T_\perp + T_\parallel\,,\\
T_\perp &= -4\pi \sum_{\lambda=\pm} \int \frac{\mathrm{d}\mathbf{k}\, j_\lambda J_\lambda}{(2\pi)^3(\omega^2 - k^2 + \mathrm{i}0)}\,,\\
T_\parallel &= -\frac{4\pi}{\omega^2}\int \frac{\mathrm{d}\mathbf{k}}{(2\pi)^3}\, j_\parallel J_\parallel\,,\\
j_\lambda &= \mathbf{j}\,\mathbf{s}^*_\lambda\,, \qquad J_\lambda = \mathbf{J}\mathbf{s}_\lambda\,, \qquad j_\parallel = \mathbf{j}\,\frac{\mathbf{k}}{k}\,, \qquad J_\parallel = \mathbf{J}\,\frac{\mathbf{k}}{k}\,.
\end{aligned}
\tag{3}
$$

Here, $T_\perp$ and $T_\parallel$ are the respective amplitudes for which the polarization of the virtual photon is perpendicular and parallel to its momentum $\mathbf{k}$. Each of the amplitudes $T_\perp$ and $T_\parallel$ can be written as a sum,

$$T_\perp = T_\perp^{(0)} + T_\perp^{(1)}\,, \qquad T_\parallel = T_\parallel^{(0)} + T_\parallel^{(1)}\,, \tag{4}$$

where $T_{\perp,\parallel}^{(0)}$ correspond to the amplitudes that do not take the interaction between the produced pair and the atomic field into account, while such an interaction is accounted for in amplitudes $T_{\perp,\parallel}^{(1)}$. In other words, the terms $T_{\perp,\parallel}^{(0)}$ correspond to the bremsstrahlung of a virtual photon decaying into a free pair. We note that $T_{\perp,\parallel}^{(0)}$ necessarily takes the interaction of an incoming particle with the atomic field into account, because a free particle cannot produce a free pair. The interaction of an incoming particle with the atomic field can be absent in amplitudes $T_{\perp,\parallel}^{(1)}$ because such an interaction is not required to emit a virtual photon that creates a pair interacting with the field. For the reader's convenience, explicit expressions for the amplitudes $T_{\perp,\parallel}^{(0)}$ and $T_{\perp,\parallel}^{(1)}$ are given in the Appendix. Here, we note only the structure of these expressions:

$$\begin{aligned}
&T_\perp^{(0)} = A(\boldsymbol{\Delta}_0)t_\perp^{(0)}\,, \qquad T_\parallel^{(0)} = A(\boldsymbol{\Delta}_0)t_\parallel^{(0)}\,,\\
&T_\perp^{(1)} = \int \mathrm{d}\boldsymbol{\Delta}_\perp\, A(\boldsymbol{\Delta}_\perp + \mathbf{p}_{2\perp})t_\perp^{(1)}(\boldsymbol{\Delta}_\perp)\,,\\
&T_\parallel^{(1)} = \int \mathrm{d}\boldsymbol{\Delta}_\perp\, A(\boldsymbol{\Delta}_\perp + \mathbf{p}_{2\perp})t_\parallel^{(1)}(\boldsymbol{\Delta}_\perp)\,,\\
&A(\boldsymbol{\Delta}) = -\frac{\mathrm{i}}{\Delta_\perp^2}\int \mathrm{d}\mathbf{r}\, \exp\bigl(-\mathrm{i}\boldsymbol{\Delta}\mathbf{r} - \mathrm{i}\chi(\rho)\bigr)\boldsymbol{\Delta}_\perp\boldsymbol{\nabla}_\perp V(r)\,,\\
&\chi(\rho) = \int_{-\infty}^{\infty}\mathrm{d}z\, V\bigl(\sqrt{z^2+\rho^2}\bigr)\,, \qquad \boldsymbol{\rho} = \mathbf{r}_\perp\,,\\
&\boldsymbol{\Delta}_0 = \mathbf{p}_2 + \mathbf{p}_3 + \mathbf{p}_4 - \mathbf{p}_1\,,
\end{aligned} \tag{5}$$

where $t_{\perp,\parallel}^{(0)}$ and $t_{\perp,\parallel}^{(1)}$ are some functions, $V(r)$ is the potential energy of the incoming particle in the atomic field, and $\mathbf{X}_\perp$ is the component of $\mathbf{X}$ perpendicular to $\mathbf{p}_1$: $\mathbf{X}_\perp = \mathbf{X} - \mathbf{p}_1(\mathbf{X}\mathbf{p}_1)/p_1^2$. Because the amplitudes $T_{\perp,\parallel}^{(0)}$ do not contain the interaction of the produced pair with the atomic field, the functions $t_{\perp,\parallel}^{(0)}$ are independent of the parameters of the atomic potential; in contrast, the functions $t_{\perp,\parallel}^{(1)}$ depend on these parameters. Thus, all the Coulomb corrections related to the interaction between the incoming particle and the atomic field are determined by the function $A(\boldsymbol{\Delta})$ alone, while the Coulomb corrections related to the interaction between the produced pair and the atomic field are determined by the functions $t_{\perp,\parallel}^{(1)}$. We note that $A(\boldsymbol{\Delta})$ also describes the Coulomb corrections to the bremsstrahlung amplitude of a real photon in an atomic field (see Ref. [41]). For $\Delta_\parallel = 0$, with $\Delta_\parallel = \boldsymbol{\Delta}\mathbf{p}_1/p_1$, the following relation is valid:

$$\begin{aligned}
A(\boldsymbol{\Delta}_\perp) &= -\frac{\mathrm{i}}{\Delta_\perp^2}\int \mathrm{d}\boldsymbol{\rho}\, \exp\bigl(-\mathrm{i}\boldsymbol{\Delta}_\perp\boldsymbol{\rho} - \mathrm{i}\chi(\rho)\bigr)\boldsymbol{\Delta}_\perp\boldsymbol{\nabla}_\perp\chi(\rho)\\
&= \mathrm{i}\int \mathrm{d}\boldsymbol{\rho}\, \exp\bigl(-\mathrm{i}\boldsymbol{\Delta}_\perp\boldsymbol{\rho} - \mathrm{i}\chi(\rho)\bigr)\,.
\end{aligned} \tag{6}$$

Therefore, $A(\boldsymbol{\Delta}_\perp)$ does not vanish in the absence of the potential, but is converted into another function:

$$A(\boldsymbol{\Delta}_\perp) \to \mathrm{i}(2\pi)^2\delta(\boldsymbol{\Delta}_\perp)\,. \tag{7}$$

Thus, in the absence of interaction between the incoming particle and the atomic field, the amplitudes $T_{\perp,\parallel}^{(1)}$ do not tend to zero [see Eqns (5)]:

$$T_{\perp,\parallel}^{(1)} \to \mathrm{i}(2\pi)^2 t_{\perp,\parallel}^{(1)}(-\mathbf{p}_{2\perp})\,. \tag{8}$$

The function $A(\boldsymbol{\Delta}_\perp)$ has the following remarkable property, which is valid for any localized potential $V(r)$ and arbitrary function $G(\boldsymbol{\Delta}_\perp)$ independent of $\mathbf{p}_{2\perp}$:

$$\int \mathrm{d}\mathbf{p}_{2\perp}\left|\int \mathrm{d}\boldsymbol{\Delta}_\perp\, A(\boldsymbol{\Delta}_\perp + \mathbf{p}_{2\perp})G(\boldsymbol{\Delta}_\perp)\right|^2 = (2\pi)^4\int \mathrm{d}\mathbf{p}_{2\perp}\bigl|G(\mathbf{p}_{2\perp})\bigr|^2\,. \tag{9}$$

Relation (9) can be easily proved using expression (6):

$$\begin{aligned}
\int \mathrm{d}\mathbf{p}_{2\perp}\left|\int \mathrm{d}\boldsymbol{\Delta}_\perp\, A(\boldsymbol{\Delta}_\perp + \mathbf{p}_{2\perp})G(\boldsymbol{\Delta}_\perp)\right|^2 &= \iint \mathrm{d}\mathbf{x}\,\mathrm{d}\mathbf{y}\, G(\mathbf{x})G^*(\mathbf{y})\\
&\times \iint \mathrm{d}\boldsymbol{\rho}_1\,\mathrm{d}\boldsymbol{\rho}_2 \exp\Bigl[\mathrm{i}\bigl(\chi(\rho_2) - \chi(\rho_1)\bigr) + \mathrm{i}\mathbf{y}\boldsymbol{\rho}_2 - \mathrm{i}\mathbf{x}\boldsymbol{\rho}_1\Bigr]\\
&\times \int \mathrm{d}\mathbf{p}_{2\perp}\exp\bigl[\mathrm{i}\mathbf{p}_{2\perp}(\boldsymbol{\rho}_2 - \boldsymbol{\rho}_1)\bigr]\,.
\end{aligned} \tag{10}$$

Integrating first over $\mathbf{p}_{2\perp}$ and then over $\boldsymbol{\rho}_1$, $\boldsymbol{\rho}_2$, and $\mathbf{y}$, we obtain Eqn (9). It is owing to Eqn (9) that the Coulomb corrections to the electroproduction amplitude coming from the interaction between the incoming particle and the atomic field have little effect on the magnitude of the cross section integrated over the momentum $\mathbf{p}_{2\perp}$. But these corrections strongly affect the differential cross section in $\mathbf{p}_{2\perp}$.

The integral representation of the function $A(\boldsymbol{\Delta})$ is very convenient for treating the screening of the nucleus Coulomb field by atomic electrons and the effect of a finite nucleus size. For $R^{-1} \gg \Delta_\perp$, $\Delta_\parallel \gg r_{\mathrm{scr}}^{-1}$, where R is the nucleus radius and r_{scr} is the screening radius, $A(\boldsymbol{\Delta})$ can be replaced by the Coulomb function

$$\begin{aligned}
A_{\mathrm{C}}(\boldsymbol{\Delta}) = &-\frac{4\pi\eta(L\Delta)^{2\mathrm{i}\eta}}{\Delta^2}\,\Gamma(1-\mathrm{i}\eta)\,\Gamma(2-\mathrm{i}\eta)\\
&\times F\left(1-\mathrm{i}\eta, \mathrm{i}\eta, 2, \frac{\Delta_\perp^2}{\Delta^2}\right),
\end{aligned} \tag{11}$$

where $F(a,b,c,x)$ is the hypergeometric function, $\Gamma(x)$ is Euler's function, and $L \sim r_{\mathrm{scr}}$. The parameter L enters only the common phase of the process, and the cross section is therefore independent of L. For $\Delta_\perp \gg \Delta_\parallel$, the function $A_{\mathrm{C}}(\boldsymbol{\Delta})$ transforms into the asymptotic form

$$A_{\mathrm{as}}(\boldsymbol{\Delta}_\perp) = -\frac{4\pi\eta(L\Delta_\perp)^{2\mathrm{i}\eta}\Gamma(1-\mathrm{i}\eta)}{\Delta_\perp^2\Gamma(1+\mathrm{i}\eta)}\,. \tag{12}$$

The differential cross section of the electroproduction process for distinct particles takes the form

$$\mathrm{d}\sigma = \frac{\alpha^2}{(2\pi)^8}\,\mathrm{d}\varepsilon_3\,\mathrm{d}\varepsilon_4\,\mathrm{d}\mathbf{p}_{2\perp}\mathrm{d}\mathbf{p}_{3\perp}\mathrm{d}\mathbf{p}_{4\perp}\frac{1}{2}\sum_{\mu_i=\pm1}\bigl|T_{\mu_1\mu_2\mu_3\mu_4}\bigr|^2\,, \tag{13}$$

where $\mu_i = \pm 1$ is the helicity of a particle with the momentum $\mathbf{p}_i$, and $\bar{\mu}_i = -\mu_i$. To describe the production of an $\mathrm{e}^+\mathrm{e}^-$ pair by a relativistic electron in an atomic field, we need to take the identity of particles into account, i.e., replace the amplitude $T_{\mu_1\mu_2\mu_3\mu_4}$ with another one, namely

$$\begin{aligned}
&\mathcal{T}_{\mu_1\mu_2\mu_3\mu_4} = T_{\mu_1\mu_2\mu_3\mu_4} - \widetilde{T}_{\mu_1\mu_2\mu_3\mu_4}\,,\\
&\widetilde{T}_{\mu_1\mu_2\mu_3\mu_4} = T_{\mu_1\mu_3\mu_2\mu_4}(\mathbf{p}_2 \leftrightarrow \mathbf{p}_3)\,.
\end{aligned} \tag{14}$$

We are now in a position to discuss differential and integral electroproduction cross sections in various cases.

3. Production of an e^+e^- pair by a relativistic electron in an atomic field

In this section, we discuss how various effects influence the differential and integral cross sections of the e^+e^- pair electroproduction by a relativistic electron in an atomic field. The section is based on Refs [36, 37]. We are interested in the magnitude of contributions from the amplitudes $T^{(0)}$ and $\widetilde{T}^{(0)}$ to the cross section (i.e., the contribution from the emission of a virtual photon transforming into an e^+e^- pair of particles that do not interact with the atomic field), the effect of interference between the amplitudes T and $\widetilde{T}$ (i.e., the importance of accounting for the identity of electrons), and the influence of Coulomb corrections related to the interaction of both the incoming particle and the produced pair with the atomic field.

We begin with the fully differential cross section. We consider the quantity

$$S = \sum_{\mu_i=\pm1} \left| \frac{\varepsilon_1 m_e^4 \mathcal{T}_{\mu_1\mu_2\mu_3\mu_4}}{\eta(2\pi)^2} \right|^2 , \qquad (15)$$

which is the dimensionless differential cross section, with m_e being the electron mass. Figure 2 shows the dependence of S on the transverse positron momentum $p_{4\perp}$ for an atom of gold ($Z = 79$) for some values of ε_i, $\mathbf{p}_{2\perp}$, and $\mathbf{p}_{3\perp}$. In this figure, the exact result (solid curve) is compared with results obtained in the following approximations:

- the lowest (Born) approximation in the parameter η (dotted curve);
- disregarding the interference between the amplitudes T and $\widetilde{T}$ (dashed-dotted curve);
- disregarding the interaction of the incoming electron with the atomic field (long-dash curve);
- disregarding the amplitudes $T^{(0)}$ and $\widetilde{T}^{(0)}$ (short-dash curve).

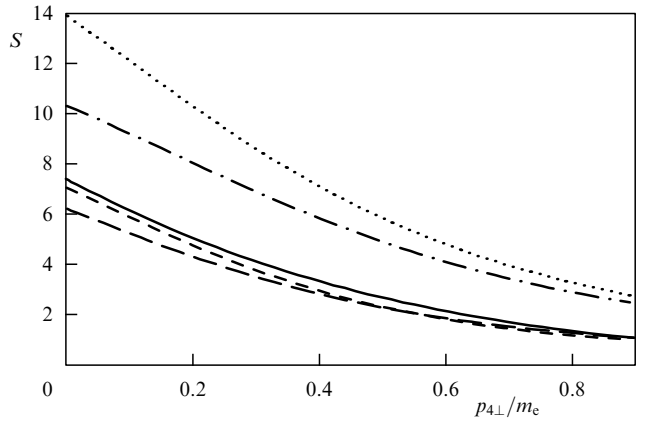

Figure 2. Quantity S as a function of $p_{4\perp}/m_e$ [see Eqn (15)] for $Z = 79$, $\varepsilon_1 = 100m_e$, $\varepsilon_2/\varepsilon_1 = 0.28$, $\varepsilon_3/\varepsilon_1 = 0.42$, $\varepsilon_4/\varepsilon_1 = 0.3$, $p_{2\perp} = 1.3m_e$, $p_{3\perp} = 0.5m_e$, $\mathbf{p}_{3\perp} \parallel \mathbf{p}_{4\perp}$; the angle between the momenta $\mathbf{p}_{2\perp}$ and $\mathbf{p}_{4\perp}$ is $\pi/2$. Shown are the exact result (solid line), the Born approximation (dotted line), the result obtained disregarding the interference between T and $\widetilde{T}$ (dashed-dotted line), the result obtained disregarding the incoming electron with the atomic field (long-dash line), and the result obtained disregarding $T^{(0)}$ and $\widetilde{T}^{(0)}$ (short-dash line).

It can be seen that the Born result differs substantially from the exact one, being almost twice as large. Accounting for interference leads to a difference of about 50%, and accounting for the interaction of the incoming electron with the atomic field changes the cross section by about 15%. The contribution of the amplitudes $T^{(0)}$ and $\widetilde{T}^{(0)}$ is noticeable, but is not large (about 5%). The influence of atomic screening is negligibly small for the parameter range shown in Fig. 2. We note that the relative contribution of the effects we are interested in to the differential cross section strongly depends on $\mathbf{p}_i$. However, in all cases, the Born cross section deviates substantially from the exact one, even for moderate values of Z.

To observe experimentally how the interaction between the incoming electron and the atomic field influences the differential electroproduction cross section, it suffices to measure the transverse momentum or the final momentum angles of one of the electrons. For the cross section $d\sigma/dp_{2\perp}$, the magnitude of this effect is large in the range $p_{2\perp}/m_e \lesssim 1$. Such an experiment seems to be well realizable for not very large $\gamma = \varepsilon_1/m_e \lesssim 100$.

Interestingly, for a polarized incoming electron, the differential cross section exact in η is characterized by asymmetry $\mathcal{A}$:

$$\mathcal{A} = \frac{S_+ - S_-}{S_+ + S_-} , \qquad S_\pm = \sum_{\mu_2\mu_3\mu_4} \left| \frac{\varepsilon_1 m_e^4 \mathcal{T}_{\pm\mu_2\mu_3\mu_4}}{\eta(2\pi)^2} \right|^2 . \qquad (16)$$

In the Born approximation, the asymmetry disappears for any momenta $\mathbf{p}_i$ owing to the relation

$$\mathcal{T}^{B}_{\mu_1\mu_2\mu_3\mu_4} = -\mu_1\mu_2\mu_3\mu_4 \left(\mathcal{T}^{B}_{\bar{\mu}_1\bar{\mu}_2\bar{\mu}_3\bar{\mu}_4} \right)^* , \qquad (17)$$

which does not hold if the Coulomb corrections are taken into account. The asymmetry $\mathcal{A}$ is shown in Fig. 3 as a function of φ_3 (the angle between $\mathbf{p}_{3\perp}$ and $\mathbf{p}_{4\perp}$) for some values of ε_i, $p_{i\perp}$, and φ_2 (the angle between $\mathbf{p}_{2\perp}$ and $\mathbf{p}_{4\perp}$). As we expect, asymmetry disappears if all momenta lie in the same plane ($\varphi_2 = 0, \pi$ and $\varphi_3 = 0, \pi$ in Fig. 3). It can be seen that the asymmetry can reach several dozen percent.

We now consider the differential cross section in the transverse electron momentum, $d\sigma/dp_{2\perp}$. This cross section is shown in Fig. 4a for $Z = 79$ (gold) and $\varepsilon_1 = 100m_e$. These results are obtained under the assumption $\varepsilon_i \gg m_e$; therefore,

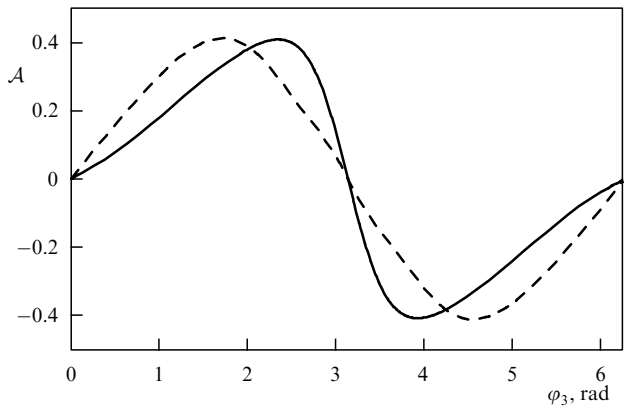

Figure 3. Asymmetry $\mathcal{A}$ [see Eqn (16)] as a function of φ_3 for $\varepsilon_2/\varepsilon_1 = 0.28$, $\varepsilon_3/\varepsilon_1 = 0.42$, $\varepsilon_4/\varepsilon_1 = 0.3$, $p_{2\perp} = 0.3m_e$, $p_{3\perp} = 0.5m_e$, $p_{4\perp} = 1.2m_e$, and $\eta = 0.6$ for $\varphi_2 = 0$ (solid line) and $\varphi_2 = \pi$ (dashed line); φ_i is the angle between $\mathbf{p}_{i\perp}$ and $\mathbf{p}_{4\perp}$. In the Born approximation, $\mathcal{A} = 0$.

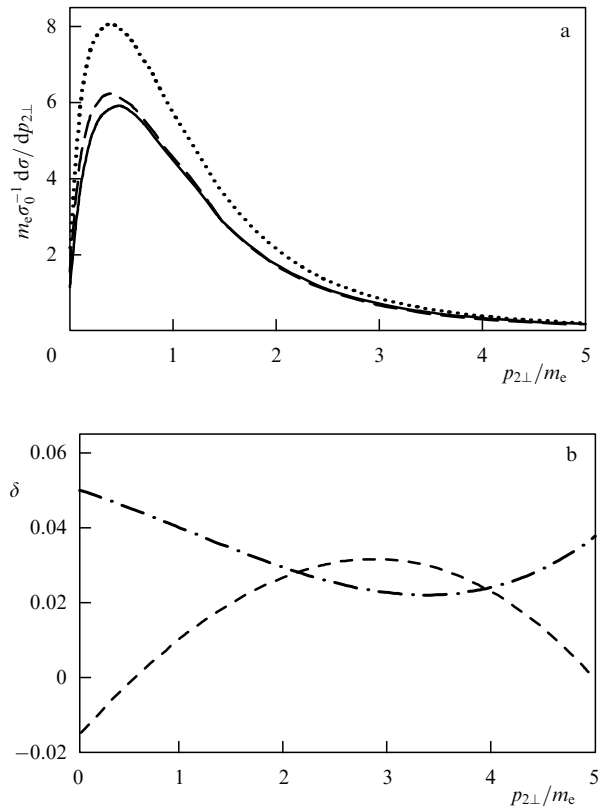

Figure 4. (a) Dependence of $d\sigma/dp_{2\perp}$ on $p_{2\perp}/m_e$ in units of $\sigma_0/m_e = \alpha^2\eta^2/m_e^3$ for $Z = 79$ and $\varepsilon_1/m_e = 100$; shown are the exact result (solid line), the Born approximation (dotted line), the result obtained without disregarding the interaction between the incoming electron and the atomic field (dashed line). (b) The quantity δ as a function of $p_{2\perp}/m_e$, where δ is the deviation of the approximate result $d\sigma/dp_{2\perp}$ from the exact one in units of exact cross section; the dashed-dotted line plots the result obtained disregarding the interference between T and $\widetilde{T}$; the dashed line plots the result obtained disregarding $T^{(0)}$ and $\widetilde{T}^{(0)}$.

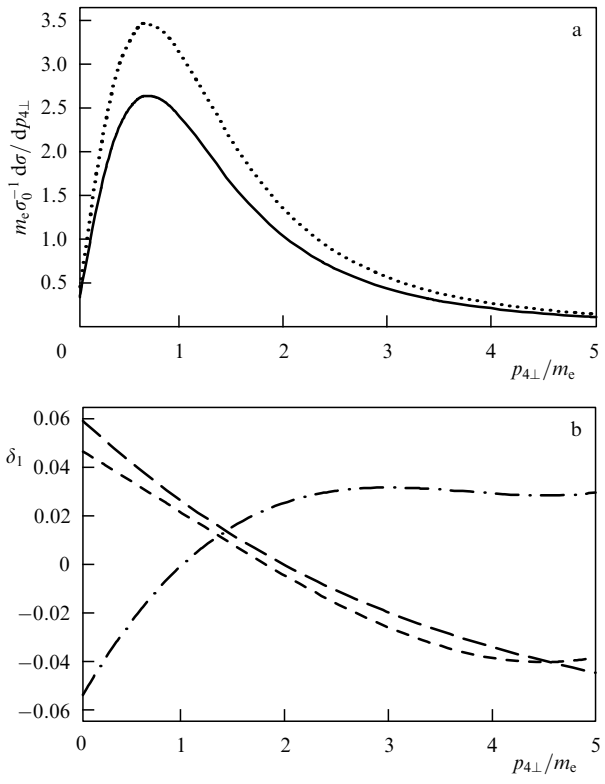

Figure 5. (a) Dependence of $d\sigma/dp_{4\perp}$ on $p_{4\perp}/m_e$ in units of $\sigma_0/m_e = \alpha^2\eta^2/m_e^3$ for $Z = 79$ and $\varepsilon_1/m_e = 100$. The solid line plots the exact result and the dotted line plots the Born approximation. (b) The quantity δ_1 (the relative deviation of the approximate result from the exact one) for $d\sigma/dp_{4\perp}$ as a function of $p_{4\perp}/m_e$. The dashed-dotted line depicts the result obtained disregarding the interference between T and $\widetilde{T}$, the long-dash line presents the result obtained without the contribution from $T^{(0)}$ and $\widetilde{T}^{(0)}$, and the short-dash line presents the result disregarding the interaction between the incoming electron and the atomic field.

the question arises as to the lower limit for integration over the energies of final particles in the computation of $d\sigma/dp_{2\perp}$. It turns out that varying the lower limit by a quantity comparable to m_e only weakly influences the final result and does not substantially modify the relation between contributions from different corrections. Figure 4a shows the result of integration over the entire kinematically allowed domain. Figure 4b shows δ, the relative deviation of the approximate result for $d\sigma/dp_{2\perp}$ computed without accounting for the amplitudes $T^{(0)}$ and $\widetilde{T}^{(0)}$ or without interference from the exact one. It can be seen that both effects make a noticeable, but not very large contribution to the cross section ($\delta \leqslant 5\%$). It follows from Fig. 4a that the exact result is markedly different from the Born approximation (the difference peaks at 50%), and taking the interaction of the incoming electron with the atomic field into account leads to a substantial reduction in the cross section at the peak ($\sim 20\%$) and a weak increase over a broad range of momenta $p_{2\perp}$ outside the peak. These deviations (positive and negative) effectively compensate each other in the cross section integrated over transverse electron momenta $p_{2\perp}$ and $p_{3\perp}$. This statement is illustrated in Fig. 5, which shows the differential cross section in the transverse positron momentum, $d\sigma/dp_{4\perp}$, for $Z = 79$ and $\varepsilon_1 = 100m_e$.

As follows from Fig. 5a, the Born approximation for $d\sigma/dp_{4\perp}$ is substantially different from the exact one (by approximately 30% at the peak). Figure 5b shows δ_1, the relative deviation of the approximate result for $d\sigma/dp_{4\perp}$ (computed disregarding the interaction between the incoming electron and the atomic field or the contribution from the amplitudes $T^{(0)}$ and $\widetilde{T}^{(0)}$ or interference) from the exact one. All values of δ_1 are significant ($\delta_1 \leqslant 6\%$). The cross section obtained without taking the interaction between the incoming electron and the atomic field into account and the cross section that include the amplitudes $T^{(0)}$ and $\widetilde{T}^{(0)}$ are very close to each other. This indicates that the Coulomb corrections related to the interaction of the incoming electron with the atomic field lead to a very small shift in $d\sigma/dp_{4\perp}$, whereas $d\sigma/dp_{2\perp}$ changes rather substantially.

We consider the total cross section σ of the process under study. This cross section is shown in Fig. 6a for $Z = 79$ as a function of ε_1/m_e. The solid line corresponds to the exact result, the dotted line depicts the Born approximation, and the dashed-dotted line shows the ultrarelativistic asymptotic behavior of the Born result [2] (the Racah formula). We note that the small difference at relatively small energies between the Born approximation and the result computed with the Racah formula is related to two factors. First, our result for the total cross section involves an uncertainty rooted in the selection of the lower limit for integration over energies. Second, the Racah formula [2] ignores the identity of electrons. It can be seen that the Born result for the total

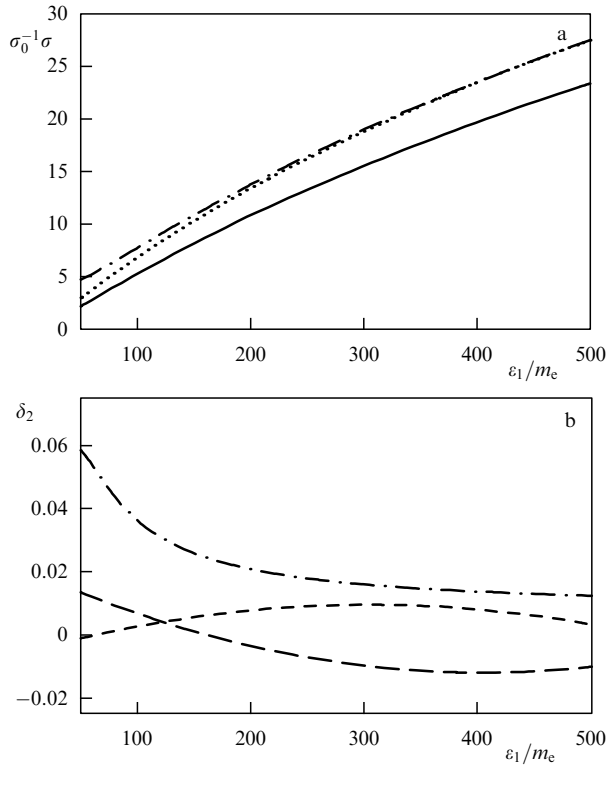

Figure 6. Total cross section σ as a function ε_1/m_e in units of $\sigma_0 = \alpha^2\eta^2/m_e^2$ for $Z = 79$. The solid line shows the exact result, the dotted line shows the Born approximation, and the dashed-dotted line shows the result obtained with the Racah formula [2]. (b) The quantity δ_2 (the deviation of the approximate result σ from the exact one in units of exact cross section) as a function of ε_1/m_e. The dashed-dotted line presents the result ignoring the interference between T and $\widetilde{T}$, the short-dash line present the result without $T^{(0)}$ and $\widetilde{T}^{(0)}$, and the long-dash line presents the result without the interaction between the incoming electron and atomic field.

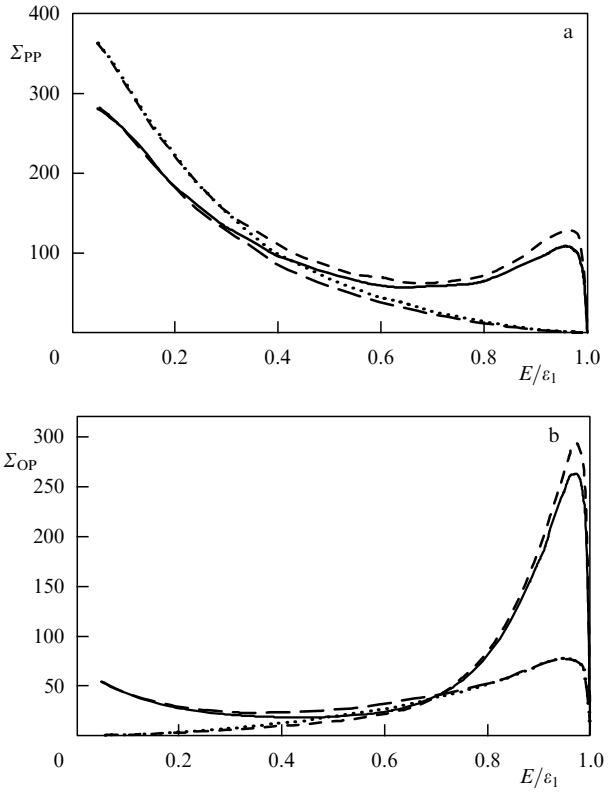

Figure 7. Spectra of (a) parapositronium $\Sigma_{PP} = S^{-1}\,d\sigma_{PP}/dE$ and (b) orthopositronium $\Sigma_{OP} = S^{-1}\,d\sigma_{OP}/dE$, where S is defined in Eqn (22) as a function of E/ε_1 for $Z = 79$ and $\varepsilon_1 = 1000\,m_e$. Shown are the exact result (solid line), the Born approximation (short-dash line), the exact result in η that takes only positronium production from a virtual photon into account (without the contribution from the exchange diagram $\widetilde{T}$) (long-dash line), and the Born result for this contribution (dotted line).

cross section differs considerably from the exact result (by more than 20% in the entire domain that is shown). Figure 6b shows the relative deviation δ_2 of the approximate result for σ from the exact one. The corrections to the total cross section due to $T^{(0)}$ and $\widetilde{T}^{(0)}$ and the Coulomb corrections due to the interaction between the incoming electron and the atomic field are small, even for moderate energies ε_1. The effect of interference, which is important at moderate energies, decreases as energy is increased.

4. Positronium production in electron–atom collisions at high energies

Using formulas obtained for differential cross sections for the electroproduction of an e^+e^- pair with given momenta, we can readily find the electroproduction cross section for positronium (the bound state of e^+ and e^-). Positronium can be produced either in a state with zero total spin (parapositronium, having the positive C-parity) or with the total spin equal to one (orthopositronium, having a negative C-parity). The electroproduction cross section σ_{PP} for parapositronium with the angular momentum $l = 0$ and principal quantum number n takes the form [26, 28]

$$d\sigma_{PP} = \frac{\alpha^2 E}{(2\pi)^5 2m_e}\left|\psi_n(0)\right|^2 dE\, d\mathbf{p}_{2\perp}\, d\mathbf{P}_\perp\, \frac{1}{2}\sum_{\mu_1\mu_2}\left|\overline{T}_{\mu_1\mu_2}\right|^2, \quad (18)$$

where E and $\mathbf{P}$ are the positronium energy and momentum, $E = (P^2 + 4m_e^2)^{1/2}$, and $\psi_n(0)$ is the positronium wave function at the origin, $|\psi_n(0)|^2 = \alpha^3 m_e^3/(8\pi n^3)$. The amplitude $\overline{T}_{\mu_1\mu_2}(\mathbf{p}_1, \mathbf{p}_2, \mathbf{P})$ is expressed in terms of the amplitude $\mathcal{T}_{\mu_1\mu_2\mu_3\mu_4}(\mathbf{p}_1, \mathbf{p}_2, \mathbf{p}_3, \mathbf{p}_4)$ [see Eqn (14)] as

$$\overline{T}_{\mu_1\mu_2}(\mathbf{p}_1, \mathbf{p}_2, \mathbf{P}) = \frac{1}{\sqrt{2}}\left[\mathcal{T}_{\mu_1\mu_2+-}\left(\mathbf{p}_1, \mathbf{p}_2, \frac{\mathbf{P}}{2}, \frac{\mathbf{P}}{2}\right) - \mathcal{T}_{\mu_1\mu_2-+}\left(\mathbf{p}_1, \mathbf{p}_2, \frac{\mathbf{P}}{2}, \frac{\mathbf{P}}{2}\right)\right]. \quad (19)$$

We now determine the total positronium production cross section

$$d\sigma_{tot} = \frac{\alpha^2 E}{(2\pi)^5 2m_e}\left|\psi_n(0)\right|^2 dE\, d\mathbf{p}_{2\perp}\, d\mathbf{P}_\perp \times \frac{1}{2}\sum_{\mu_i=\pm1}\left|\mathcal{T}_{\mu_1\mu_2\mu_3\mu_4}\left(\mathbf{p}_1, \mathbf{p}_2, \frac{\mathbf{P}}{2}, \frac{\mathbf{P}}{2}\right)\right|^2. \quad (20)$$

Then the production cross section for orthopositronium is expressed as

$$d\sigma_{OP} = d\sigma_{tot} - d\sigma_{PP}. \quad (21)$$

Figure 7 shows the dependence of parapositronium and orthopositronium spectra $\Sigma_{PP} = S^{-1}d\sigma_{PP}/dE$ and $\Sigma_{OP} =$

$S^{-1}\,\mathrm{d}\sigma_{\mathrm{OP}}/\mathrm{d}E$ on E/ε_1, where

$$S=\frac{\eta^2}{Em_{\mathrm{e}}^5}\left|\psi_n(0)\right|^2, \tag{22}$$

for $Z=79$ and $\varepsilon_1=1000\,m_{\mathrm{e}}$. There are two contributions to the production amplitude of positronium from an electron with a momentum $\mathbf{p}_3$ and a positron with a momentum $\mathbf{p}_4$. In the first case, positronium is formed from the electron and positron produced by a virtual photon (the amplitude T), and in the second case the positron is captured by the electron emitting a virtual photon (the exchange amplitude $\widetilde{T}$). Figure 7 shows that for $E\sim\varepsilon_1$, the exact result (the solid line) is substantially different from the result obtained by disregarding the exchange diagram (the long-dash line). In both cases, the result exact in η is substantially different from the Born approximation (the short-dash and dotted lines, respectively). We note that the result exact in η for the spectrum of positronium production was obtained in Ref. [40] without taking the exchange contribution into account. Our results shown in Fig. 7 by the long-dash line agree with those in Ref. [40].

5. Production of an e^+e^- pair by a relativistic muon in an atomic field

The e^+e^- pair production by a relativistic heavy particle in an atomic field is a very important process because its cross section is even larger than the bremsstrahlung cross section for a heavy particle in the atomic field. This is why it contributes substantially to energy losses of heavy particles in detectors. The cross section of e^+e^- pair production by a relativistic heavy particle in an atomic field was calculated in the Born approximation many years ago [1, 2]. In this approximation, the cross section depends on the atom charge number Z and the charge number of the heavy particle Z_{p} (the ratio of its charge to that of the proton) as $Z^2Z_{\mathrm{p}}^2$. The interaction between the heavy particle and the atomic field was ignored in [1, 2]. Later, the Coulomb corrections related to the interaction of the e^+e^- pair with the atomic field were obtained in Refs [10, 11] using plane waves for the particle wave function and Coulomb wave functions for the electron and positron. The results in Refs [10, 11] for the cross section are therefore exact in the parameter $Z\alpha$, but depend on Z_{p} as Z_{p}^2 (Z_{p} enters only the amplitude of a virtual photon). The authors of Refs [10, 11] obtained the cross section both differential in the heavy particle final momenta and integrated over these momenta. In the latter case, the cross section was also obtained in another framework (see Refs [15, 16] and reviews [44, 45]), by computing the cross section for a given impact parameter ρ of a heavy particle relative to the atom center, which means ignoring the interaction between the heavy particle and the atomic field. The result was then integrated over the impact parameters. Thus, the final result corresponds to the cross section integrated over the momenta of a heavy particle.

We note that the energy ω of the produced pair e^+e^-, which makes the main contribution to the cross section, is much smaller than the energy of a heavy particle. As a consequence, the process cross section does not depend on the spin and mass m_{p} of the heavy particle but depends on the relativistic factor $\gamma=\varepsilon_{\mathrm{p}}/m_{\mathrm{p}}$, where ε_{p} is the heavy particle energy. The final formulas for electroproduction cross sections of an e^+e^- pair by a muon or light nucleus coincide (with due regard for the respective charge number).

In our recent study [38], we computed the differential cross section of e^+e^- pair production in an atomic field by a relativistic muon or light nucleus taking the interaction between the heavy particle and the atomic field into account. The results obtained are exact in both parameters $\eta=Z\alpha$ and $\eta_{\mathrm{p}}=Z_{\mathrm{p}}Z\alpha=Z_{\mathrm{p}}\eta$. It was shown that the cross section differential in the final particle momentum strongly depends on η_{p}, contradicting well-accepted views. For light nuclei in the field of a heavy atom, this parameter can be large, $\eta_{\mathrm{p}}\gtrsim 1$. However, the cross section integrated over the final momenta of the heavy particle does not depend on η_{p}. Experimental observation of a strong dependence of the cross section differential in $\mathbf{p}_{2\perp}$ on η_{p} for not very large values of the relativistic factor γ seems to be fully plausible.

The differential process cross section is given by Eqn (13), and the Feynman diagram for the amplitude T in the Furry representation is shown in Fig. 1. The leading contribution to the cross section comes from the range of electron and positron energies $\varepsilon_{3,4}\lesssim\gamma m_{\mathrm{e}}$, where $\gamma=\varepsilon_1/m_{\mathrm{p}}\gg 1$, whence $\omega/\varepsilon_1\lesssim m_{\mathrm{e}}/m_{\mathrm{p}}\ll 1$.

We first consider the process in the Coulomb field and then discuss the effect of screening. In the e^+e^- pair electroproduction by a heavy relativistic particle, the contribution $T^{(0)}$ is not large compared to $T^{(1)}$. The contribution $T^{(1)}$ is the sum of contributions, $T^{(1)}=T_\perp+T_\parallel$, which in the Coulomb field take the form

$$T_\perp=\frac{8\mathrm{i}\eta}{\omega}\left|\Gamma(1-\mathrm{i}\eta)\right|^2\int\frac{\mathrm{d}\boldsymbol{\Delta}_\perp A_{\mathrm{as}}(\boldsymbol{\Delta}_\perp+\mathbf{p}_{2\perp})}{(Q^2+\Delta_{0\parallel}^2)M^2(\omega^2/\gamma^2+\Delta_\perp^2)}\left(\frac{\xi_2}{\xi_1}\right)^{\mathrm{i}\eta}\mathcal{M},$$

$$\mathcal{M}=-\frac{\delta_{\mu_3\bar{\mu}_4}}{\omega}\left[\varepsilon_3(\mathbf{e}^*_{\mu_3}\boldsymbol{\Delta}_\perp)(\mathbf{e}_{\mu_3}\mathbf{I}_1)-\varepsilon_4(\mathbf{e}^*_{\mu_4}\boldsymbol{\Delta}_\perp)(\mathbf{e}_{\mu_4}\mathbf{I}_1)\right]$$
$$+\mu_3\delta_{\mu_3\mu_4}\frac{m_{\mathrm{e}}}{\sqrt{2}}(\mathbf{e}^*_{\mu_3}\boldsymbol{\Delta}_\perp)\,I_0\,, \tag{23}$$

$$T_\parallel=-\frac{8\mathrm{i}\eta\varepsilon_3\varepsilon_4}{\omega^3}\left|\Gamma(1-\mathrm{i}\eta)\right|^2\int\frac{\mathrm{d}\boldsymbol{\Delta}_\perp A_{\mathrm{as}}(\boldsymbol{\Delta}_\perp+\mathbf{p}_{2\perp})}{(Q^2+\Delta_{0\parallel}^2)M^2}\left(\frac{\xi_2}{\xi_1}\right)^{\mathrm{i}\eta}I_0\delta_{\mu_3\bar{\mu}_4},$$

where $\omega=\varepsilon_3+\varepsilon_4$, $\mathbf{e}_\lambda=(\mathbf{e}_x+\mathrm{i}\lambda\mathbf{e}_y)/\sqrt{2}$, $\mathbf{e}_x$ and $\mathbf{e}_y$ are unit vectors orthogonal to the vector $\mathbf{p}_1$ and to each other, and the function $A_{\mathrm{as}}(\boldsymbol{\Delta}_\perp)$ is defined by Eqn (12) with the replacement $\eta\to\eta_{\mathrm{p}}$. The following notation is adopted in Eqn (23):

$$\begin{aligned}
&\Delta_{0\parallel}=-\frac{1}{2}\left[\frac{\omega}{\gamma^2}+\frac{\omega(m_{\mathrm{e}}^2+\boldsymbol{\zeta}^2)}{\varepsilon_3\varepsilon_4}+\frac{\boldsymbol{\delta}^2}{\omega}+\frac{p_{2\perp}^2}{\varepsilon_1}\right],\\
&M^2=m_{\mathrm{e}}^2+\frac{\varepsilon_3\varepsilon_4}{\gamma^2}+\frac{\varepsilon_3\varepsilon_4}{\omega^2}\,\Delta_\perp^2\,,\\
&\mathbf{Q}=\boldsymbol{\Delta}_\perp-\boldsymbol{\delta}\,,\qquad \mathbf{q}_1=\frac{\varepsilon_3}{\omega}\mathbf{Q}-\boldsymbol{\zeta}\,,\qquad \mathbf{q}_2=\frac{\varepsilon_4}{\omega}\mathbf{Q}+\boldsymbol{\zeta}\,,\\
&\boldsymbol{\zeta}=\frac{\varepsilon_4}{\omega}\,\mathbf{p}_{3\perp}-\frac{\varepsilon_3}{\omega}\,\mathbf{p}_{4\perp}\,,\qquad \boldsymbol{\delta}=\mathbf{p}_{3\perp}+\mathbf{p}_{4\perp}\,,\\
&I_0=(\xi_1-\xi_2)\,F(x)+(\xi_1+\xi_2-1)(1-x)\,\frac{F'(x)}{\mathrm{i}\eta}\,,\\
&\mathbf{I}_1=(\xi_1\mathbf{q}_1+\xi_2\,\mathbf{q}_2)\,F(x)+(\xi_1\mathbf{q}_1-\xi_2\,\mathbf{q}_2)(1-x)\,\frac{F'(x)}{\mathrm{i}\eta}\,,\\
&\xi_1=\frac{M^2}{M^2+q_1^2}\,,\qquad \xi_2=\frac{M^2}{M^2+q_2^2}\,,\qquad x=1-\frac{Q^2\xi_1\xi_2}{M^2}\,,\\
&F(x)=F(\mathrm{i}\eta,-\mathrm{i}\eta,1,x)\,,\qquad F'(x)=\frac{\partial F(x)}{\partial x}\,,
\end{aligned} \tag{24}$$

where $F(a,b,c,x)$ is the hypergeometric function. To take screening into account, we have to replace $A_{\mathrm{as}}(\boldsymbol{\Delta}_\perp)\to A(\boldsymbol{\Delta}_\perp)$

(see our paper [36]) in Eqn (23),

$$A(\boldsymbol{\Delta}_\perp) = \mathrm{i}\int \mathrm{d}\boldsymbol{\rho}\,\exp\left(-\mathrm{i}\boldsymbol{\Delta}_\perp\boldsymbol{\rho} - \mathrm{i}Z_\mathrm{p}\chi(\rho)\right),$$
$$\chi(\rho) = \int_{-\infty}^{\infty} \mathrm{d}z\, V\left(\sqrt{z^2+\rho^2}\right), \tag{25}$$

where $V(r)$ is the atomic potential, and multiply the integrand in Eqn (23) by the atomic form factor $F_\mathrm{a}((\boldsymbol{\Delta}_\perp - \boldsymbol{\delta})^2 + \Delta_{0\|}^2)$. In the absence of interaction between the heavy charged particle and the atomic field, the influence of screening on the process cross section is studied in Ref. [4]. In this case, screening is important for $\gamma \gg m_\mathrm{e} r_\mathrm{scr} \sim Z^{-1/3}/\alpha$. For the cross section differential in $p_{2\perp}$, the effect of screening is essential for $\gamma \gg (\omega/m_\mathrm{e}) m_\mathrm{e} r_\mathrm{scr} \gg m_\mathrm{e} r_\mathrm{scr}$. Therefore, up to very high values of γ for the heavy particle, we can use $A_\mathrm{as}(\boldsymbol{\Delta})$ in (12) instead of $A(\boldsymbol{\Delta})$ in (25), yet accounting for the atomic form factor F_a. We skip the details of how screening influences the electroproduction process.

In terms of the variables $\boldsymbol{\zeta}$, $\boldsymbol{\delta}$, and $\mathbf{p}_{2\perp}$ [see relations (24)], the leading contribution to the total cross section comes from the integration domain ζ, δ, $p_{2\perp} \lesssim m_\mathrm{e}$, and $\omega \lesssim m_\mathrm{e}\gamma$. In this domain, $\omega/\varepsilon_1 \lesssim m_\mathrm{e}/m_\mathrm{p}$ and $p_{2\perp}/\varepsilon_1 \ll p_{3\perp}/\varepsilon_3$, $p_{4\perp}/\varepsilon_4$, which means that the angle between the momenta $\mathbf{p}_2$ and $\mathbf{p}_1$ is much smaller than the angles between $\mathbf{p}_3$, $\mathbf{p}_4$, and $\mathbf{p}_1$. We consider the cross section integrated over $\mathbf{p}_{2\perp}$. In this case, we can disregard the last term $p_{2\perp}^2/\varepsilon_1$ in $\Delta_{0\|}$ [see Eqn (24)] because it is small compared to the other terms (its relative contribution to $\Delta_{0\|}$ is of the order of $m_\mathrm{e}/m_\mathrm{p}$). Then the variable $\mathbf{p}_{2\perp}$ is present in the expression for the amplitude T only as the argument of the function $A_\mathrm{as}(\boldsymbol{\Delta}_\perp + \mathbf{p}_{2\perp})$ [see Eqns (23)]. Using Eqn (9), we find that the cross section integrated over $\mathbf{p}_{2\perp}$ does not depend on the parameter η_p (the cross section is insensitive to the interaction between the heavy particle and the atomic field). Therefore, the cross section integrated over $\mathbf{p}_{2\perp}$ can be obtained based on amplitudes computed in the limit $\eta_\mathrm{p} \to 0$ with the help of Eqn (8). The cross section $\mathrm{d}\sigma_0$ in this limit is given by Eqn (13) with the change $T \to T_0 = T_{0\perp} + T_{0\|}$, where

$$T_{0\perp} = -\frac{32\pi^2\eta\left|\Gamma(1-\mathrm{i}\eta)\right|^2 \mathcal{M}_0}{\omega\Delta_0^2 M^2(\omega^2/\gamma^2 + p_{2\perp}^2)}\left(\frac{\xi_2}{\xi_1}\right)^{\mathrm{i}\eta},$$
$$\mathcal{M}_0 = \frac{\delta_{\mu_3\bar{\mu}_4}}{\omega}\left[\varepsilon_3(\mathbf{e}^*_{\mu_3}\mathbf{p}_{2\perp})(\mathbf{e}_{\mu_3}\mathbf{I}_1) - \varepsilon_4(\mathbf{e}^*_{\mu_4}\mathbf{p}_{2\perp})(\mathbf{e}_{\mu_4}\mathbf{I}_1)\right]$$
$$- \mu_3\delta_{\mu_3\mu_4}\frac{m_\mathrm{e}}{\sqrt{2}}(\mathbf{e}^*_{\mu_3}\mathbf{p}_{2\perp})I_0\,, \tag{26}$$
$$T_{0\|} = \frac{32\pi^2\eta\varepsilon_3\varepsilon_4\left|\Gamma(1-\mathrm{i}\eta)\right|^2}{\omega^3\Delta_0^2 M^2}\left(\frac{\xi_2}{\xi_1}\right)^{\mathrm{i}\eta} I_0\delta_{\mu_3\bar{\mu}_4}\,.$$

Here, the notation agrees with that in Eqn (23) after the replacement $\boldsymbol{\Delta}_\perp \to -\mathbf{p}_{2\perp}$. Result (26) agrees with the respective result in Ref. [10].

Although the cross section integrated over $\mathbf{p}_{2\perp}$ does not depend on η_p, the differential cross section in $\mathbf{p}_{2\perp}$ is strongly dependent on this parameter. This statement is based on the results of computations shown in Fig. 8, where the quantity

$$\Sigma = \frac{\mathrm{d}\sigma}{S\,\mathrm{d}p_{2\perp}\,\mathrm{d}\varepsilon_3\,\mathrm{d}\varepsilon_4}\,, \qquad S = \frac{(Z_\mathrm{p}\alpha)^2}{\omega^2 m_\mathrm{e}^3}\,, \tag{27}$$

which is the cross section differential in $\mathbf{p}_{2\perp}$ (in units of S), integrated over $\mathbf{p}_{3\perp}$ and $\mathbf{p}_{4\perp}$, is given as a function of $p_{2\perp}$ for $\omega = m_\mathrm{e}\gamma/4$, $\varepsilon_3 = \varepsilon_4 = \omega/2$, $\gamma = 100$, $Z = 79$, and several values of Z_p.

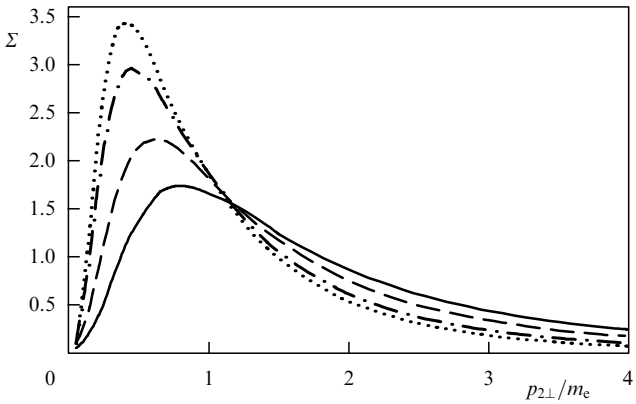

Figure 8. Dependence of Σ on $p_{2\perp}/m_\mathrm{e}$ [see Eqn (27)] for $\omega = m_\mathrm{e}\gamma/4$, $\varepsilon_3 = \varepsilon_4 = \omega/2$, $\gamma = 100$, and $Z = 79$ for $Z_\mathrm{p} = 3$ (solid line), $Z_\mathrm{p} = 2$ (dashed line), $Z_\mathrm{p} = 1$ (dashed-dotted line), and $Z_\mathrm{p} \to 0$ (disregarding the interaction between the heavy particle and the atomic field) (dotted line).

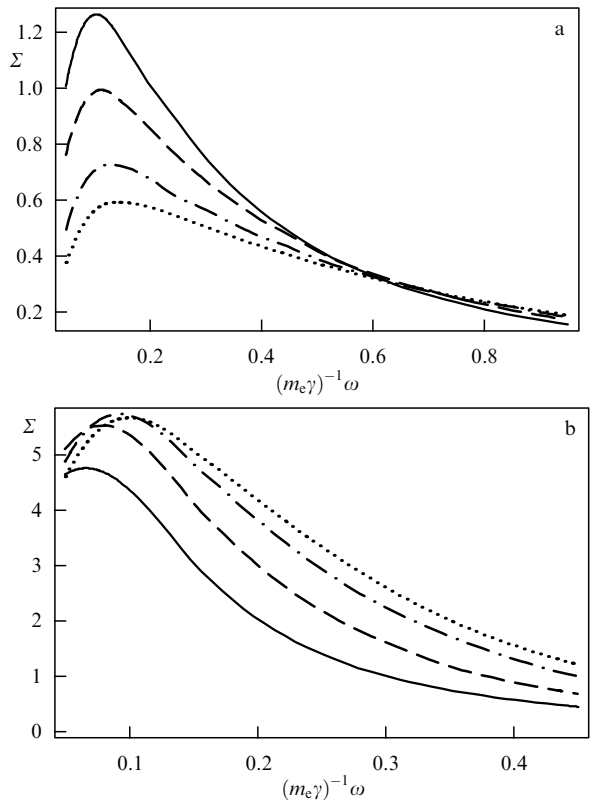

Figure 9. Dependence of Σ on $\omega/(m_\mathrm{e}\gamma)$ [see Eqn (27)] for (a) $p_{2\perp}/m_\mathrm{e} = 2$ and (b) $p_{2\perp}/m_\mathrm{e} = 0.5$, $\varepsilon_3 = \varepsilon_4$, $\gamma = 100$, and $Z = 79$ for $Z_\mathrm{p} = 3$ (solid line), $Z_\mathrm{p} = 2$ (dashed line), $Z_\mathrm{p} = 1$ (dashed-dotted line), and $Z_\mathrm{p} \to 0$ (disregarding the interaction between the heavy particle and the atomic field) (dotted line).

It can be seen that the influence of the interaction between the heavy particle and the atomic field on the cross section differential in $\mathbf{p}_{2\perp}$ is very strong. For small values of $p_{2\perp}/m_\mathrm{e}$, the cross section exact in η_p is substantially lower than the cross section obtained in the limit $\eta_\mathrm{p} \to 0$. For large values of $p_{2\perp}/m_\mathrm{e}$, the relation between these cross sections reverses. The integral $\int_0^\infty \Sigma\,\mathrm{d}p_{2\perp}$ is independent of η_p, as it should.

The dependence of Σ on $\omega/(m_\mathrm{e}\gamma)$ for $p_{2\perp}/m_\mathrm{e} = 2$ is shown in Fig. 9a, and for $p_{2\perp}/m_\mathrm{e} = 0.5$ in Fig. 9b for $\varepsilon_3 = \varepsilon_4$, $\gamma = 100$, $Z = 79$, and several values of Z_p. It can be seen that the dependence of Σ on Z_p is very strong for any $\omega/(m_\mathrm{e}\gamma)$.

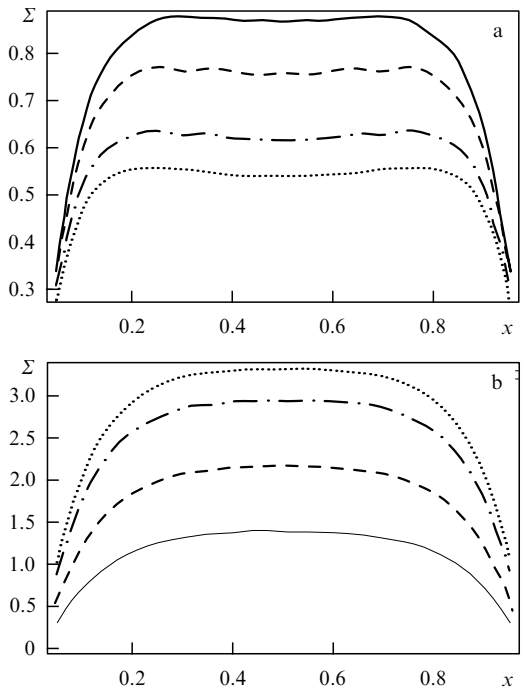

Figure 10. Dependence of Σ on $x = \varepsilon_3/\omega$ [see Eqn (27)] for $\omega = m_e\gamma/4$, $\gamma = 100$, $Z = 79$, (a) $p_{2\perp}/m_e = 2$ and (b) $p_{2\perp}/m_e = 0.5$ for $Z_p = 3$ (solid line), $Z_p = 2$ (dashed line), $Z_p = 1$ (dashed-dotted line), and $Z_p \to 0$ (disregarding the interaction between the heavy particle and the atomic field) (dotted line).

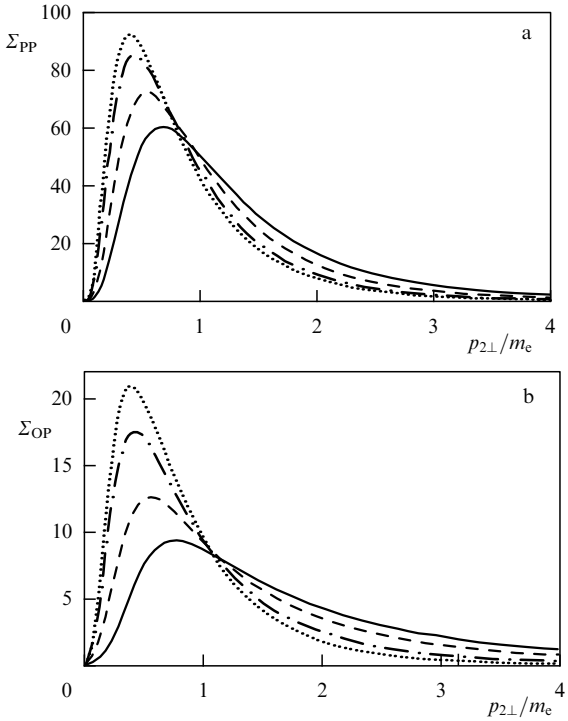

Figure 11. Dependence of (a) Σ_{PP} and (b) Σ_{OP} on $p_{2\perp}/m_e$ [see Eqn (32)] for $E = m_e\gamma/4$, $\gamma = 100$, and $Z = 79$ for $Z_p = 3$ (solid line), $Z_p = 2$ (dashed line), $Z_p = 1$ (dashed-dotted line), and $Z_p \to 0$ (disregarding the interaction between the heavy particle and the atomic field) (dotted line).

The dependence of Σ on $x = \varepsilon_3/\omega$ for $\omega = m_e\gamma/4$, $\gamma = 100$, $Z = 79$, and several values of Z_p is plotted in Fig. 10a for $p_{2\perp}/m_e = 2$, and in Fig. 10b for $p_{2\perp}/m_e = 0.5$. As in the preceding cases, taking the interaction between the heavy particle and the atomic field into account is very important for the differential cross section.

The situation with the dependence of the electroproduction cross section on η_p is reminiscent of that with the dependence of Coulomb corrections to the relativistic muon bremsstrahlung cross section in an atomic field (see Ref. [42]). The Coulomb correction to the bremsstrahlung cross section and the differential cross section in the muon and photon momenta lead to substantial deviations from the result obtained in the Born approximation. However, this correction reduces to zero when integrated over the momentum of the muon (or photon).

To observe the strong dependence of the differential process cross section on the parameter η_p, one needs to measure the final momentum angles of the final heavy particle. The angle between the momenta $\mathbf{p}_2$ and $\mathbf{p}_1$ is substantially smaller than the angles between the momenta $\mathbf{p}_3$, $\mathbf{p}_4$, and $\mathbf{p}_1$. However, experiments for moderate values of the relativistic factor γ seem to be possible.

6. Positronium and muonium production in collisions of relativistic muons with atoms

The electroproduction cross section σ_{PP} for parapositronium, characterized by the angular momentum $l = 0$ and the principal quantum number n, in a collision of a heavy particle with an atom takes the form [cf. Eqn (18)]

$$\mathrm{d}\sigma_{PP} = \frac{\alpha^2 E}{(2\pi)^5 2m_e} \left|\psi_n(0)\right|^2 \mathrm{d}E\, \mathrm{d}\mathbf{p}_{2\perp}\, \mathrm{d}\mathbf{P}_\perp \left|\overline{T}\right|^2, \tag{28}$$

where E and $\mathbf{P}$ are the positronium energy and momentum, $E = (P^2 + 4m_e^2)^{1/2}$, $\psi_n(0)$ is the positronium wave function at the origin, and $|\psi_n(0)|^2 = \alpha^3 m_e^3/(8\pi n^3)$. The amplitude $\overline{T}(\mathbf{p}_1, \mathbf{p}_2, \mathbf{P})$ is expressed in terms of the amplitude $T_{\mu_3\mu_4}(\mathbf{p}_1, \mathbf{p}_2, \mathbf{p}_3, \mathbf{p}_4)$ [see Eqn (23)] as

$$\overline{T}(\mathbf{p}_1, \mathbf{p}_2, \mathbf{P}) = \frac{1}{\sqrt{2}} \left[T_{+-}\left(\mathbf{p}_1, \mathbf{p}_2, \frac{\mathbf{P}}{2}, \frac{\mathbf{P}}{2}\right) - T_{-+}\left(\mathbf{p}_1, \mathbf{p}_2, \frac{\mathbf{P}}{2}, \frac{\mathbf{P}}{2}\right)\right]. \tag{29}$$

We recall that the process amplitude is independent of the heavy particle spin. The total positronium electroproduction cross section $\mathrm{d}\sigma_{tot}$ is given by the formula

$$\mathrm{d}\sigma_{tot} = \frac{\alpha^2 E}{(2\pi)^5 2m_e} \left|\psi_n(0)\right|^2 \mathrm{d}E\, \mathrm{d}\mathbf{p}_{2\perp}\, \mathrm{d}\mathbf{P}_\perp \times \sum_{\mu_{3,4}=\pm 1} \left| T_{\mu_3\mu_4}\left(\mathbf{p}_1, \mathbf{p}_2, \frac{\mathbf{P}}{2}, \frac{\mathbf{P}}{2}\right)\right|^2. \tag{30}$$

The orthopositronium production cross section is then expressed as

$$\mathrm{d}\sigma_{OP} = \mathrm{d}\sigma_{tot} - \mathrm{d}\sigma_{PP}. \tag{31}$$

Figure 11 shows the dependence of dimensionless quantities Σ_{PP} and Σ_{OP} on $p_{2\perp}$,

$$\Sigma_{PP} = \frac{\mathrm{d}\sigma_{PP}}{S\, \mathrm{d}p_{2\perp}\, \mathrm{d}E}, \quad \Sigma_{OP} = \frac{\mathrm{d}\sigma_{OP}}{S\, \mathrm{d}p_{2\perp}\, \mathrm{d}E}, \quad S = \frac{\eta^2}{Em_e^6} \left|\psi_n(0)\right|^2, \tag{32}$$

for $Z = 79$, $\gamma = 100$, $E = m_e\gamma/4$, and several values of Z_p (the heavy particle charge in units of $|e|$).

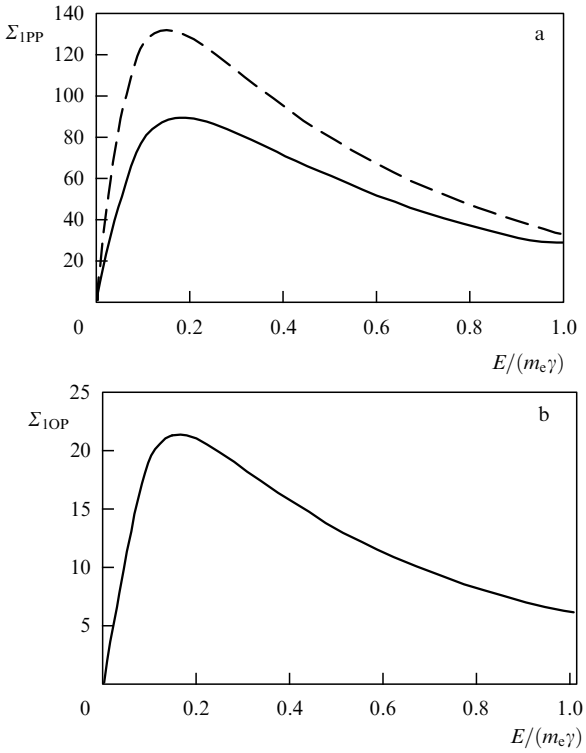

Figure 12. Dependence of (a) Σ_{1PP} and (b) Σ_{1OP} on $E/(m_e\gamma)$ [see Eqn (33)] for $\gamma = 100$ and $Z = 79$; the exact result in η (solid line) and the Born approximation (dashed line). The production cross section for orthopositronium is zero in the Born approximation.

It can be seen that just as for an unbound electron and positron, taking the interaction between the heavy particle and the atomic field into account substantially affects the positronium electroproduction cross section differential in $p_{2\perp}$. Furthermore, the orthopositronium production cross section is substantially lower than for parapositronium. This is due to the preservation of C-parity, because for the production of orthopositronium an exchange of at least two photons with the atomic field is needed, while one-photon exchange is sufficient for parapositronium.

The positronium production cross section integrated over $p_{2\perp}$ does not change if the interaction between the heavy particle and the atomic field is taken into account. The dependence of positronium spectra on E/m_e,

$$\Sigma_{1PP} = \frac{d\sigma_{PP}}{m_e S\, dE}, \qquad \Sigma_{1OP} = \frac{d\sigma_{OP}}{m_e S\, dE}, \tag{33}$$

where S is defined in Eqn (32), is plotted in Fig. 12. These spectra do not depend on Z_p.

In addition to positronium production in collisions of a heavy charged particle with an atom, a bound state of a heavy particle and a positron can form, for example, muonium (a μ^-e^+ atom). The cross section of this process is

$$d\sigma_{\mu e} = \frac{\alpha^2\gamma}{(2\pi)^5}\left|\psi_n(0)\right|^2 dE\, d\mathbf{p}_{3\perp}\, d\mathbf{P}_\perp \times \sum_{\mu_{3,4}=\pm1}\left|T_{\mu_3\mu_4}\left(\mathbf{p}_1, \mathbf{P}, \mathbf{p}_3, \frac{m_e}{m_\mu}\mathbf{P}\right)\right|^2, \tag{34}$$

where E and $\mathbf{P}$ are the muonium energy and momentum, $E = (P^2 + m_\mu^2)^{1/2}$, $\psi_n(0)$ is the muonium wave function at the origin, and $|\psi_n(0)|^2 = \alpha^3 m_e^3/(\pi n^3)$. Because the process amplitude is independent of the heavy-particle spin, the cross sections of muonium production with spin zero and spin one are respectively equal to $\sigma_{\mu e}/4$ and $3\sigma_{\mu e}/4$. The dependence of the cross section (in units of S_1)

$$\Sigma_{\mu e} = \frac{d\sigma_{\mu e}}{S_1\, dp_{3\perp}\, dE}, \qquad S_1 = \frac{\eta^2}{\gamma m_e^7}\left|\psi_n(0)\right|^2,$$

on $p_{3\perp}/m_e$ is shown in Fig. 13. We note that $|\psi_n(0)|^2$ for positronium is 1/8 that for muonium.

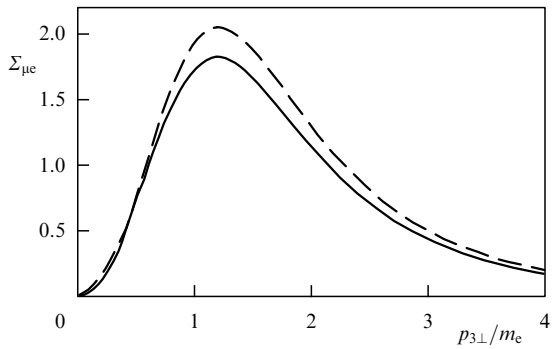

Figure 13. Dependence of $\Sigma_{\mu e}$ on $p_{3\perp}/m_e$ for $\gamma = 100$, $Z = 79$, and $\varepsilon_3 = \gamma m_e/4$. The respective solid and dashed lines show the result exact in η and the Born approximation.

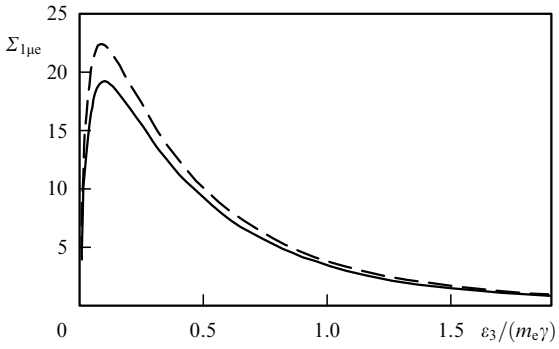

Figure 14. Dependence of $\Sigma_{1\mu e}$ on $\varepsilon_3/(m_e\gamma)$ for $\gamma = 100$ and $Z = 79$. The respective solid and dashed lines show the result exact in η and the Born approximation.

Because the energy conservation law requires that $E = m_\mu\gamma - \varepsilon_3$, the muonium spectrum has a peak in the range $E \sim m_\mu\gamma$ of the width $\Delta E \sim m_e\gamma$, as indicated in Fig. 14, where the dependence of the spectrum $\Sigma_{1\mu e} = d\sigma_{\mu e}/m_e S_1\, d\varepsilon_3$ on $\varepsilon_3/m_e\gamma$ is plotted.

We note that the total positronium production cross section is amplified only logarithmically (by about $\ln\gamma$ times) compared to the total muonium production cross section. However, $|\psi_n(0)|^2$ for muonium is eight times larger than for positronium.

7. Production of a $\mu^+\mu^-$ pair by a relativistic electron in an atomic field

The process of $\mu^+\mu^-$ pair production by a relativistic electron in an atomic field has a particular feature that the Coulomb corrections to the cross section (the difference between the results exact in η and those obtained in the

Born approximation), related to the interaction of the $\mu^+\mu^-$ pair with the atomic field, are strongly suppressed by the nuclear form factor [46], as in the case of photoproduction of a $\mu^+\mu^-$ pair [47]. The Coulomb corrections due to the interaction between the electron and the atomic field were discussed in our recent work [39]. It turned out that these corrections can significantly change the process cross section differential in the electron final momentum angles, just as for the e^+e^- pair electroproduction in an atomic field by a relativistic heavy particle [38] and a relativistic electron [36, 37]. But the cross section integrated over the final momentum angles of the final electron does not change if interaction between the electron and the atomic field is considered.

We note that in the process considered in this section, taking nucleus screening by atomic electrons into account is important only for very large energies,

$$\varepsilon_1 \gtrsim \frac{m_\mu^2}{\alpha Z^{1/3} m_e} \sim 1\,\text{TeV}\,,$$

and can typically be disregarded. However, accounting for the finite nucleus size R is indispensable. The reason is that for heavy atoms, the Compton length of the muon $\lambda_\mu = 1/m_\mu$ is shorter than R. To simplify computations, we consider the nucleus potential $V(r)$ in the form

$$V(r) = -\frac{\eta}{\sqrt{r^2 + R^2}}\,. \tag{35}$$

For this potential, the form factor $F(Q^2)$ and the function $A(\boldsymbol{\Delta}_\perp)$ [see Eqn (6)] are expressed as

$$\begin{aligned} F(Q^2) &= QRK_1(QR)\,,\\ A(\boldsymbol{\Delta}_\perp) &= A_{\text{as}}(\boldsymbol{\Delta}_\perp)\,\frac{(\Delta_\perp R)^{1-i\eta}\,K_{1-i\eta}(\Delta_\perp R)}{2^{-i\eta}\Gamma(1-i\eta)}\,, \end{aligned} \tag{36}$$

where $K_\nu(x)$ is the modified Bessel function of the second kind and $A_{\text{as}}(\boldsymbol{\Delta}_\perp)$ is defined in Eqn (12). We remark that the difference between the results obtained for the real and model form factors does not exceed 10% (see Ref. [28], where the cross section is considered in the Born approximation). The weak dependence of results on the form of the potential does not affect the qualitative analysis of the importance of Coulomb corrections due to the interaction between the electron and the atomic field.

We consider the dimensionless quantity

$$\Sigma = \frac{\mathrm{d}\sigma}{S\,\mathrm{d}p_{2\perp}\,\mathrm{d}\varepsilon_3\,\mathrm{d}\varepsilon_4}\,, \qquad S = \frac{\eta^2}{\omega^2 m_\mu^2 m_e}\,, \tag{37}$$

which is the cross section integrated over $\mathbf{p}_{3\perp}$ and $\mathbf{p}_{4\perp}$, measured in units of S. The dependence of this quantity on $p_{2\perp}$ is plotted in Fig. 15 for $\omega = \varepsilon_1/2$, $\varepsilon_3 = \varepsilon_4 = \omega/2$, $\varepsilon_1 = 50\,m_\mu$, and $Z = 79$. It can be seen that the effect of interaction between the electron and the atomic field is large for the cross section differential in $p_{2\perp}$. In the region $p_{2\perp} \sim m_e$, the exact cross section is substantially smaller than the one found in the Born approximation (the deviation is about 20–30%). For $p_{2\perp} \gg m_e$, the exact solution is larger than the Born one (the deviation is about 10%). However, the Coulomb corrections to the cross section integrated over $p_{2\perp}$, i.e., to the quantity

$$\Sigma_1 = \frac{1}{m_e}\int_0^\infty \Sigma\,\mathrm{d}p_{2\perp}\,, \tag{38}$$

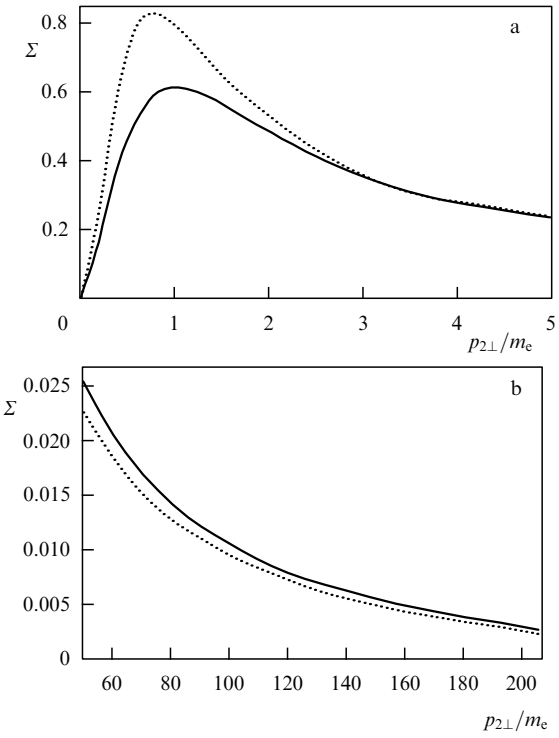

Figure 15. Dependence of Σ on $p_{2\perp}/m_e$ [see Eqn (37)] for $\omega = \varepsilon_1/2$, $\varepsilon_3 = \varepsilon_4 = \omega/2$, $\varepsilon_1 = 50m_\mu$, and $Z = 79$. The respective solid and dashed lines present the exact result and the Born approximation.

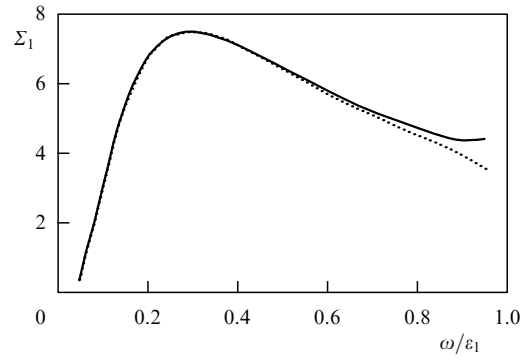

Figure 16. Dependence of Σ_1 on ω/ε_1 [see Eqn (38)] for $\varepsilon_3 = \varepsilon_4 = \omega/2$, $\varepsilon_1 = 50m_\mu$, and $Z = 79$. The respective solid and dashed lines show the exact result and the result without the contribution from $T^{(0)}$.

are strongly suppressed. Figure 16 presents the dependence of Σ_1 on ω/ε_1, where the exact result practically coincides with the Born one for all $\omega = \varepsilon_3 + \varepsilon_4$. It is of interest to consider the relative contribution of the amplitude $T^{(0)}$ to the cross section. For $\omega \ll \varepsilon_1$, the amplitude $T^{(0)}$, in contrast to the amplitude $T^{(1)}$, is suppressed by the factor ω/ε_1. Hence, the contribution of $T^{(0)}$ to the cross section is only important for $\omega \sim \varepsilon_1$. This conclusion follows from the results of computations shown in Fig. 16, where the function Σ_1 computed without the contribution from $T^{(0)}$ is plotted by a dotted curve.

Taking the amplitude $T^{(0)}$ into account leads to asymmetry in the differential cross section under permutation of the momenta of μ^+ and μ^-, $\mathbf{p}_4 \leftrightarrow \mathbf{p}_3$. Because of the

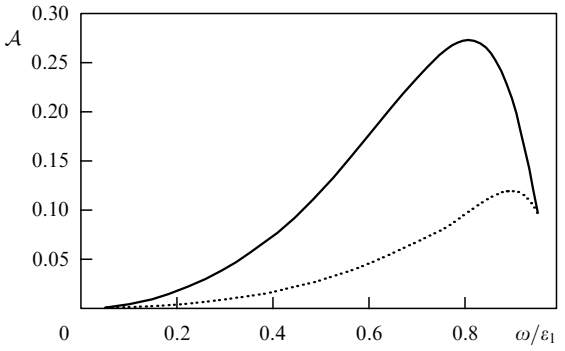

Figure 17. Dependence of $\mathcal{A}$ on ω/ε_1 [see Eqn (40)] for $\varepsilon_1 = 50m_\mu$, $\varepsilon_3 = \varepsilon_4 = \omega/2$, $\mathbf{p}_{3\perp} \| -\mathbf{p}_{4\perp}$, $p_{4\perp} = m_\mu$, and $Z = 79$; the exact result for $p_{3\perp} = 2.5m_\mu$ (solid line) and $p_{3\perp} = 0.5m_\mu$ (dotted line).

relations

$$T^{(0)}_{\mu_1\mu_2\mu_3\mu_4}(\mathbf{p}_1,\mathbf{p}_2,\mathbf{p}_3,\mathbf{p}_4) = T^{(0)}_{\mu_1\mu_2\mu_4\mu_3}(\mathbf{p}_1,\mathbf{p}_2,\mathbf{p}_4,\mathbf{p}_3)\,,$$
$$T^{(1)}_{\mu_1\mu_2\mu_3\mu_4}(\mathbf{p}_1,\mathbf{p}_2,\mathbf{p}_3,\mathbf{p}_4) = -T^{(1)}_{\mu_1\mu_2\mu_4\mu_3}(\mathbf{p}_1,\mathbf{p}_2,\mathbf{p}_4,\mathbf{p}_3)\,, \tag{39}$$

asymmetry in the cross section is caused by interference of the amplitudes $T^{(0)}$ and $T^{(1)}$. We consider the cross section integrated over $\mathbf{p}_{2\perp}$, $\mathrm{d}\sigma(\mathbf{p}_3,\mathbf{p}_4)$, and define the asymmetry as

$$\mathcal{A} = \frac{\mathrm{d}\sigma(\mathbf{p}_3,\mathbf{p}_4) - \mathrm{d}\sigma(\mathbf{p}_4,\mathbf{p}_3)}{\mathrm{d}\sigma(\mathbf{p}_3,\mathbf{p}_4) + \mathrm{d}\sigma(\mathbf{p}_4,\mathbf{p}_3)}\,. \tag{40}$$

Figure 17 presents the dependence of $\mathcal{A}$ on ω/ε_1 for several values of $\mathbf{p}_3$ and $\mathbf{p}_4$. In can be seen that the asymmetry can reach several dozen percent for $\omega \sim \varepsilon_1$.

The charge asymmetry accompanying the $\mu^+\mu^-$ photoproduction in an atomic field was studied in [49]. Asymmetry in the cross section occurs if the first semiclassical correction to the process amplitude is taken into account. The cross section computed in the leading semiclassical approximation does not exhibit this asymmetry. A question arises as to whether a beam of relativistic electrons can be used as a source of equivalent photons to observe the charge asymmetry in photoproduction due to the correction to the leading term of the semiclassical approximation. Because the charge asymmetry due to the interference of the amplitudes $T^{(0)}$ and $T^{(1)}$ is large for $\omega \sim \varepsilon_1$, observing charge asymmetry due to the first semiclassical correction to the amplitude of $\mu^+\mu^-$ pair production by a virtual photon in the electroproduction process can be problematic.

8. Production of paradimuonium by a relativistic electron in an atomic field

Using formulas obtained for the differential cross sections of electroproduction of μ^+ and μ^- with given momenta $\mathbf{p}_3$ and $\mathbf{p}_4$, we can readily find the electroproduction cross section for dimuonium (the bound state of μ^+ and μ^-). In this process, dimuonium is produced mostly in the state with the total spin zero (paradimuonium with positive C-parity), because in this case the amplitude $T^{(1)}$ is governed by only a single exchange by a virtual photon between the $\mu^+\mu^-$ pair and the atomic center. Production of orthodimuonium (negative C-parity and the total spin one) requires either the exchange by two virtual photons between $\mu^+\,\mu^-$ and the atomic center, which is suppressed by the form factor in the amplitude $T^{(1)}$, or the contribution of the amplitude $T^{(0)}$, which is small compared to $T^{(1)}$.

The electroproduction cross section σ_{PD} for paradimuonium with the angular momentum $l = 0$ and the principal quantum number n takes the form [26, 28]

$$\mathrm{d}\sigma_{\mathrm{PD}} = \frac{\alpha^2 E}{(2\pi)^5 2m_\mu}\left|\psi_n(0)\right|^2 \mathrm{d}E\,\mathrm{d}\mathbf{p}_{2\perp}\,\mathrm{d}\mathbf{P}_\perp\,\frac{1}{2}\sum_{\mu_1\mu_2}|\overline{T}_{\mu_1\mu_2}|^2\,, \tag{41}$$

where E and $\mathbf{P}$ are the dimuonium energy and momentum, $E = (P^2 + 4m_\mu^2)^{1/2}$, $\psi_n(0)$ is the dimuonium wave function at the origin, and $|\psi_n(0)|^2 = \alpha^3 m_\mu^3/(8\pi n^3)$. The amplitude $\overline{T}_{\mu_1\mu_2}(\mathbf{p}_1,\mathbf{p}_2,\mathbf{P})$ is expressed in terms of the amplitude $T_{\mu_1\mu_2\mu_3\mu_4}(\mathbf{p}_1,\mathbf{p}_2,\mathbf{p}_3,\mathbf{p}_4)$ as

$$\overline{T}_{\mu_1\mu_2}(\mathbf{p}_1,\mathbf{p}_2,\mathbf{P}) = \frac{1}{\sqrt{2}}\left[T_{\mu_1\mu_2+-}\left(\mathbf{p}_1,\mathbf{p}_2,\frac{\mathbf{P}}{2},\frac{\mathbf{P}}{2}\right) - T_{\mu_1\mu_2-+}\left(\mathbf{p}_1,\mathbf{p}_2,\frac{\mathbf{P}}{2},\frac{\mathbf{P}}{2}\right)\right]. \tag{42}$$

For the amplitude $\overline{T}_{\mu_1\mu_2}$, we find

$$\overline{T}_{\mu_1\mu_2} = \frac{4\sqrt{2}\,\mathrm{i}\eta\varepsilon_1}{E}\int\frac{\mathrm{d}\boldsymbol{\Delta}_\perp\,A(\boldsymbol{\Delta}_\perp + \mathbf{p}_{2\perp})\,F(Q^2 + \Delta_{0\|}^2)}{(Q^2 + \Delta_{0\|}^2)M^2(m_\mathrm{e}^2E^2 + \varepsilon_1^2\Delta_\perp^2)}\,\mathcal{M}\,,$$
$$\mathcal{M} = -\mu_1\delta_{\mu_1\mu_2}\left[\varepsilon_1(\mathbf{e}^*_{\mu_1}\boldsymbol{\Delta}_\perp)(\mathbf{e}_{\mu_1}\mathbf{Q}) - \varepsilon_2(\mathbf{e}_{\mu_1}\boldsymbol{\Delta}_\perp)(\mathbf{e}^*_{\mu_1}\mathbf{Q})\right] + \delta_{\mu_1\bar{\mu}_2}\frac{m_\mathrm{e}E^2}{\sqrt{2}\varepsilon_1}(\mathbf{e}_{\mu_1}\mathbf{Q})\,, \tag{43}$$
$$M^2 = m_\mu^2 + \frac{E^2m_\mathrm{e}^2}{4\varepsilon_1\varepsilon_2} + \frac{\varepsilon_1}{4\varepsilon_2}\,\Delta_\perp^2\,, \qquad \mathbf{Q} = \boldsymbol{\Delta}_\perp + \mathbf{p}_{1\perp} - \mathbf{P}_\perp\,.$$

The electroproduction cross section of paradimuonium has properties analogous to those of the electroproduction of unbound μ^+ and μ^-: the cross section differential in transverse momenta $p_{2\perp}$ contains large Coulomb corrections, contrary to accepted views [19, 20, 30, 46]. To illustrate this statement, Fig. 18 shows the dependence of the dimensionless quantity Σ_{PD} on $p_{2\perp}$,

$$\Sigma_{\mathrm{PD}} = \frac{\mathrm{d}\sigma_{\mathrm{PD}}}{S_{\mathrm{PD}}\,\mathrm{d}p_{2\perp}\,\mathrm{d}E}\,, \qquad S_{\mathrm{PD}} = \frac{\eta^2}{Em_\mu^5m_\mathrm{e}}\left|\psi_n(0)\right|^2\,, \tag{44}$$

for $Z = 79$ and $\varepsilon_1 = 50\,m_\mu$.

It can be seen that the exact result is smaller than the Born one by about 20% near the peak. In the wide region $m_\mathrm{e} \ll p_{2\perp} \lesssim m_\mu$, the exact result is about 10% higher than that of the Born approximation. Just as in other cases, the exact cross section coincides with the Born one after integration over $p_{2\perp}$, shown in Fig. 19, which plots the dependence of the spectrum on E/ε_1,

$$\Sigma_{1\mathrm{PD}} = \frac{\mathrm{d}\sigma_{\mathrm{PD}}}{m_\mathrm{e}S_{\mathrm{PD}}\,\mathrm{d}E}\,,$$

for $Z = 79$ and $\varepsilon_1 = 50m_\mu$. This dependence is very similar to that of Σ_1 on ω/ε_1 in Fig. 16.

We note that in addition to the production of dimuonium, muonium (the $\mathrm{e}^-\mu^+$ atom) can also be produced in interaction of a relativistic electron with an atomic field. However, the cross section of this process is much smaller than that of dimuonium production because $|\psi_n(0)|^2$ for dimuonium is

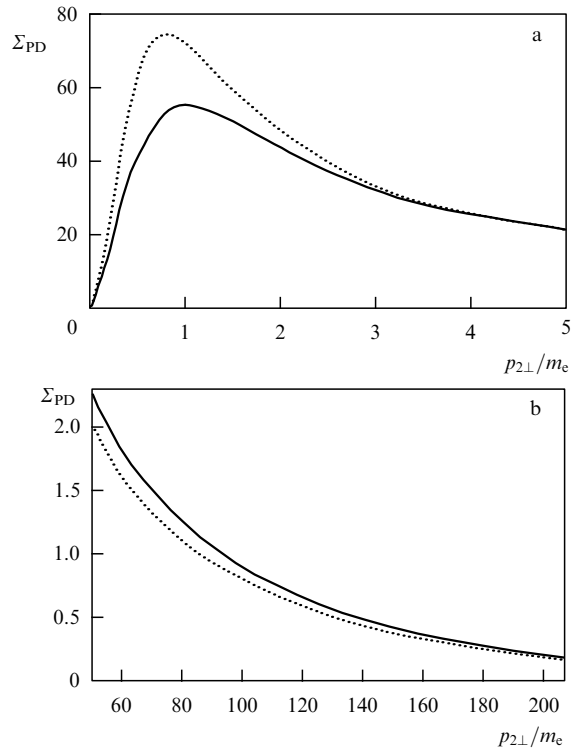

Figure 18. Dependence of $\Sigma_{\rm PD}$ on $p_{2\perp}/m_{\rm e}$ [see Eqns (44)] for $\omega = \varepsilon_1/2$, $\varepsilon_1 = 50\,m_\mu$, and $Z = 79$. The respective solid and dashed lines present the exact result and the Born approximation.

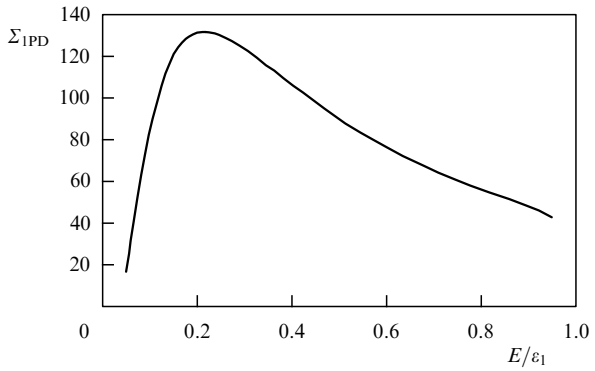

Figure 19. The dependence of $\Sigma_{\rm 1PD}$ [see Eqn (27)] on E/ε_1 for $\varepsilon_1 = 50\,m_\mu$ and $Z = 79$.

much larger than its muonium counterpart (their ratio is $m_\mu^3/(2m_{\rm e})^3$).

9. Conclusions

We presented the most recent results pertaining to the electroproduction of e^+e^- and $\mu^+\mu^-$ pairs by a relativistic electron and also the production of positronium and dimuonium in an atomic field. Furthermore, we considered the process of electroproduction of an unbound e^+e^- pair and positronium by a heavy relativistic particle (muon or light nucleus), as well as the electroproduction of an $e^+\mu^-$ atom. Special attention was paid to taking the interaction of all particles with the atomic field into account, which has become possible by resorting to the method of semiclassical Green's functions, which allows expressing solutions of the Dirac equation in an arbitrary external field in a simple form. With this method, we can readily account for the screening of the nucleus field by atomic electrons and the effect of finite nucleus size. It was shown that contrary to the commonly accepted views, taking the interaction of an incoming particle with the atomic field essentially modifies the differential cross section of the process in all cases. Experimental observation of this effect does not seem to be a very complicated task. It turns out, however, that the interaction of the incoming particle with the atomic field does not affect the magnitude of the cross section integrated over the final momenta of this particle.

This study was supported by the Russian Science Foundation (grant no. 14-50-00080).

10. Appendix

We explicitly write the amplitude T of electroproduction of a pair of particles with masses m_1 by a relativistic particle with a mass m_2 in an atomic field (see the Feynman diagram in Fig. 1). The connection between the amplitude T and the differential cross section is given by Eqn (13). The amplitude T is the sum of four contributions

$$T = T_\perp^{(0)} + T_\parallel^{(0)} + T_\perp^{(1)} + T_\parallel^{(1)}\,,$$

where

$$\begin{aligned}
T_\perp^{(0)} &= \frac{8\pi\varepsilon_3\varepsilon_4 A(\boldsymbol{\Delta}_0)}{m_2^2\omega^2 + \varepsilon_3^2\varepsilon_4^2\theta_{34}^2}\left\{\delta_{\mu_1\mu_2}\delta_{\mu_3\bar{\mu}_4}\left[\frac{\varepsilon_3}{\omega^2}(\mathbf{e}^*_{\mu_3}\mathbf{X})(\mathbf{e}_{\mu_3}\boldsymbol{\theta}_{34})\right.\right.\\
&\times(\varepsilon_1\delta_{\mu_1\mu_3} + \varepsilon_2\delta_{\mu_1\mu_4}) - \frac{\varepsilon_4}{\omega^2}(\mathbf{e}^*_{\mu_4}\mathbf{X})(\mathbf{e}_{\mu_4}\boldsymbol{\theta}_{34})(\varepsilon_1\delta_{\mu_1\mu_4} + \varepsilon_2\delta_{\mu_1\mu_3})\Big]\\
&- \frac{m_1\mu_1}{\sqrt{2}\varepsilon_1\varepsilon_2}R\delta_{\mu_1\bar{\mu}_2}\delta_{\mu_3\bar{\mu}_4}(\mathbf{e}_{\mu_1}\boldsymbol{\theta}_{34})(-\varepsilon_3\delta_{\mu_1\mu_3} + \varepsilon_4\delta_{\mu_1\mu_4})\\
&+ \frac{m_2\mu_3}{\sqrt{2}\varepsilon_3\varepsilon_4}\,\delta_{\mu_1\mu_2}\delta_{\mu_3\mu_4}(\mathbf{e}^*_{\mu_3}\mathbf{X})(\varepsilon_1\delta_{\mu_3\mu_1} + \varepsilon_2\delta_{\mu_3\bar{\mu}_1})\\
&+ \frac{m_1 m_2\omega^2}{2\varepsilon_1\varepsilon_2\varepsilon_3\varepsilon_4}R\delta_{\mu_1\bar{\mu}_2}\delta_{\mu_3\mu_4}\delta_{\mu_1\mu_3}\Big\}\,,\\
T_\parallel^{(0)} &= -\frac{8\pi}{\omega^2}A(\boldsymbol{\Delta}_0)R\delta_{\mu_1\mu_2}\delta_{\mu_3\bar{\mu}_4}\,.
\end{aligned} \tag{45}$$

Here, $\mu_i = \pm 1$ denotes the helicity of the ith particle with the momentum $\mathbf{p}_i$, $\bar{\mu}_i = -\mu_i$, $\omega = \varepsilon_3 + \varepsilon_4$, $\boldsymbol{\theta}_{ij} = \mathbf{p}_{i\perp}/\varepsilon_i - \mathbf{p}_{j\perp}/\varepsilon_j$, the function $A(\boldsymbol{\Delta})$ is defined in Eqn (5), and the following notation is introduced:

$$\begin{aligned}
&\boldsymbol{\Delta}_0 = \mathbf{p}_2 + \mathbf{p}_3 + \mathbf{p}_4 - \mathbf{p}_1\,, \qquad \boldsymbol{\Delta}_{0\perp} = \varepsilon_2\boldsymbol{\theta}_{21} + \varepsilon_3\boldsymbol{\theta}_{31} + \varepsilon_4\boldsymbol{\theta}_{41}\,,\\
&\Delta_{0\parallel} = -\frac{1}{2}\left[\omega\left(\frac{m_1^2}{\varepsilon_1\varepsilon_2} + \frac{m_2^2}{\varepsilon_3\varepsilon_4}\right) + \varepsilon_2\theta_{21}^2 + \varepsilon_3\theta_{31}^2 + \varepsilon_4\theta_{41}^2\right],\\
&R = \frac{1}{d_1 d_2}\left[\boldsymbol{\Delta}_{0\perp}^2(\varepsilon_1 + \varepsilon_2) - 2\varepsilon_1\varepsilon_2\,\boldsymbol{\theta}_{21}\boldsymbol{\Delta}_{0\perp}\right],\\
&\mathbf{X} = \frac{1}{d_1}(\varepsilon_3\boldsymbol{\theta}_{23} + \varepsilon_4\boldsymbol{\theta}_{24}) + \frac{1}{d_2}(\varepsilon_3\boldsymbol{\theta}_{31} + \varepsilon_4\boldsymbol{\theta}_{41})\,,\\
&d_1 = \omega\varepsilon_1\left(\frac{m_1^2}{\varepsilon_1\varepsilon_2} + \frac{m_2^2}{\varepsilon_3\varepsilon_4}\right) + \varepsilon_2\varepsilon_3\theta_{23}^2 + \varepsilon_2\varepsilon_4\theta_{24}^2 + \varepsilon_3\varepsilon_4\theta_{34}^2\,,\\
&d_2 = \omega\varepsilon_2\left(\frac{m_1^2}{\varepsilon_1\varepsilon_2} + \frac{m_2^2}{\varepsilon_3\varepsilon_4}\right) + \varepsilon_2\varepsilon_3\theta_{31}^2 + \varepsilon_2\varepsilon_4\theta_{41}^2 + (\varepsilon_3\boldsymbol{\theta}_{31} + \varepsilon_4\boldsymbol{\theta}_{41})^2\,.
\end{aligned} \tag{46}$$

The contributions $T_{\perp}^{(1)}$ and $T_{\parallel}^{(1)}$ are expressed as

$$
\begin{aligned}
T_{\perp}^{(1)} &= \frac{8\mathrm{i}\eta\varepsilon_1}{\omega}\left|\Gamma(1-\mathrm{i}\eta)\right|^2 \\
&\quad\times\int\frac{\mathrm{d}\boldsymbol{\Delta}_\perp\, A(\boldsymbol{\Delta}_\perp+\mathbf{p}_{2\perp})F(Q^2+\Delta_{0\parallel}^2)}{(Q^2+\Delta_{0\parallel}^2)M^2(m_1^2\omega^2+\varepsilon_1^2\Delta_\perp^2)}\left(\frac{\xi_2}{\xi_1}\right)^{\mathrm{i}\eta}\mathcal{M}\,, \\
\mathcal{M} &= -\frac{\delta_{\mu_1\mu_2}\delta_{\mu_3\bar{\mu}_4}}{\omega}\left[\varepsilon_1(\varepsilon_3\delta_{\mu_1\mu_3}-\varepsilon_4\delta_{\mu_1\mu_4})(\mathbf{e}^*_{\mu_1}\boldsymbol{\Delta}_\perp)(\mathbf{e}_{\mu_1}\mathbf{I}_1)\right. \\
&\quad\left.+\,\varepsilon_2(\varepsilon_3\delta_{\mu_1\bar{\mu}_3}-\varepsilon_4\delta_{\mu_1\bar{\mu}_4})(\mathbf{e}_{\mu_1}\boldsymbol{\Delta}_\perp)(\mathbf{e}^*_{\mu_1}\mathbf{I}_1)\right] \\
&\quad+\,\delta_{\mu_1\bar{\mu}_2}\delta_{\mu_3\bar{\mu}_4}\frac{m_1\omega\mu_1}{\sqrt{2}\varepsilon_1}(\varepsilon_3\delta_{\mu_1\mu_3}-\varepsilon_4\delta_{\mu_1\mu_4})(\mathbf{e}_{\mu_1}\mathbf{I}_1) \\
&\quad+\,\delta_{\mu_1\mu_2}\delta_{\mu_3\mu_4}\frac{m_2\mu_3}{\sqrt{2}}(\varepsilon_1\delta_{\mu_1\mu_3}+\varepsilon_2\delta_{\mu_1\bar{\mu}_3})\,\mathbf{e}^*_{\mu_3}\boldsymbol{\Delta}_\perp I_0 \\
&\quad-\frac{m_1m_2\omega^2}{2\varepsilon_1}\delta_{\mu_1\bar{\mu}_2}\delta_{\mu_3\mu_4}\delta_{\mu_1\mu_3}I_0\,, \\
T_{\parallel}^{(1)} &= -\frac{8\mathrm{i}\eta\varepsilon_3\varepsilon_4}{\omega^3}\left|\Gamma(1-\mathrm{i}\eta)\right|^2 \\
&\quad\times\int\frac{\mathrm{d}\boldsymbol{\Delta}_\perp\, A(\boldsymbol{\Delta}_\perp+\mathbf{p}_{2\perp})F(Q^2+\Delta_{0\parallel}^2)}{(Q^2+\Delta_{0\parallel}^2)M^2}\left(\frac{\xi_2}{\xi_1}\right)^{\mathrm{i}\eta}I_0\delta_{\mu_1\mu_2}\delta_{\mu_3\bar{\mu}_4}\,,
\end{aligned}
\tag{47}
$$

where $\omega=\varepsilon_3+\varepsilon_4$, $\mathbf{e}_\lambda=(\mathbf{e}_x+\mathrm{i}\lambda\mathbf{e}_y)/\sqrt{2}$, $\mathbf{e}_x$ and $\mathbf{e}_y$ are unit vectors orthogonal to $\mathbf{p}_1$ and to each other, and the function $A(\boldsymbol{\Delta}_\perp)$ is defined in Eqn (6). The following notation is used:

$$
\begin{aligned}
&M^2=m_2^2+\frac{\varepsilon_3\varepsilon_4}{\varepsilon_1\varepsilon_2}m_1^2+\frac{\varepsilon_1\varepsilon_3\varepsilon_4}{\varepsilon_2\omega^2}\,\Delta_\perp^2\,, \\
&\mathbf{Q}=\boldsymbol{\Delta}_\perp-\mathbf{p}_{3\perp}-\mathbf{p}_{4\perp}\,,\qquad \mathbf{q}_1=\frac{\varepsilon_3}{\omega}\mathbf{Q}-\boldsymbol{\zeta}\,, \\
&\mathbf{q}_2=\frac{\varepsilon_4}{\omega}\mathbf{Q}+\boldsymbol{\zeta}\,,\qquad \boldsymbol{\zeta}=\frac{\varepsilon_3\varepsilon_4}{\omega}\boldsymbol{\theta}_{34}\,, \\
&I_0=(\xi_1-\xi_2)F(x)+(\xi_1+\xi_2-1)(1-x)\,\frac{F'(x)}{\mathrm{i}\eta}\,, \\
&\mathbf{I}_1=(\xi_1\mathbf{q}_1+\xi_2\mathbf{q}_2)F(x)+(\xi_1\mathbf{q}_1-\xi_2\mathbf{q}_2)(1-x)\,\frac{F'(x)}{\mathrm{i}\eta}\,, \\
&\xi_1=\frac{M^2}{M^2+q_1^2}\,,\quad \xi_2=\frac{M^2}{M^2+q_2^2}\,,\quad x=1-\frac{Q^2\xi_1\xi_2}{M^2}\,, \\
&F(x)=F(\mathrm{i}\eta,-\mathrm{i}\eta,1,x)\,,\quad F'(x)=\frac{\partial F(x)}{\partial x}\,,
\end{aligned}
\tag{48}
$$

with $F(a,b,c,x)$ being the hypergeometric function.

References

1. Bhabha H J *Proc. R. Soc. Lond. A* **152** 559 (1935)
2. Racah G *Nuovo Cimento* **14** 93 (1937)
3. Block M M, King D T, Wada W W *Phys. Rev.* **96** 1627 (1954)
4. Murota T, Veda A, Tanaka H *Prog. Theor. Phys.* **16** 482 (1956)
5. Johnson E G (Jr.) *Phys. Rev.* **140** B1005 (1965)
6. Brodsky S J, Ting S C C *Phys. Rev.* **145** 1018 (1966)
7. Bjorken J D, Chen M C *Phys. Rev.* **154** 1335 (1967)
8. Henry R G *Phys. Rev.* **154** 1534 (1967)
9. Homma S et al. *Proc. Phys. Soc. Jpn.* **3** 1230 (1974)
10. Nikishov A I, Pichkurov N V *Sov. J. Nucl. Phys.* **35** 561 (1982); *Yad. Fiz.* **35** 964 (1982)
11. Ivanov D Yu et al. *Phys. Lett. B* **442** 453 (1998)
12. Segev B, Wells J C *Phys. Rev. A* **57** 1849 (1998)
13. Baltz A J, McLerran L *Phys. Rev. C* **58** 1679 (1998)
14. Eichmann U et al. *Phys. Rev. A* **59** 1223 (1999)
15. Ivanov D Yu, Schiller A, Serbo V G *Phys. Lett. B* **454** 155 (1999)
16. Lee R N, Milstein A I *Phys. Rev. A* **61** 032103 (2000)
17. Beranek T, Merkel H, Vanderhaeghen M *Phys. Rev. D* **88** 015032 (2013)
18. Baier V N, Synakh V S *Sov. Phys. JETP* **14** 1122 (1962); *Zh. Eksp. Teor. Fiz.* **41** 1576 (1961)
19. Kotkin G L et al. *Phys. Rev. C* **59** 2734 (1999)
20. Ginzburg I F et al. *Phys. Rev. C* **58** 3565 (1998)
21. Brodsky S J, Lebed R F *Phys. Rev. Lett.* **102** 213401 (2009)
22. Chen Y, Zhuang P, arXiv:1204.4389
23. Banburski A, Schuster P *Phys. Rev. D* **86** 093007 (2012)
24. Ellis S C, Bland-Hawthorn J *Phys. Rev. D* **91** 123004 (2015)
25. Lamm H, PhD Dissertation (Tempe, AZ: Arizona State Univ., 2016)
26. Olsen H A *Phys. Rev. D* **33** 2033 (1986)
27. Bilenkii S M et al. *Sov. J. Nucl. Phys.* **10** 469 (1970); *Yad. Fiz.* **10** 812 (1969)
28. Meledin G V, Serbo V G, Slivkov A K *JETP Lett.* **13** 68 (1971); *Pis'ma Zh. Eksp. Teor. Fiz.* **13** 98 (1971)
29. Holvik E, Olsen H A *Phys. Rev. D* **35** 2124 (1987)
30. Arteaga-Romero N, Carimalo C, Serbo V G *Phys. Rev. A* **62** 032501 (2000)
31. Bogomyagkov A et al. *EPJ Web Conf.* **181** 01032 (2018)
32. Hansson Adrian P et al. "Status of the Heavy Photon search experiment at Jefferson Laboratory", https://www.jlab.org/exp_prog/proposals/12/C12-11-006.pdf
33. REDTOP Experiment, http://redtop.fnal.gov/
34. Itahashi T et al. *JPS Conf. Proc.* **8** 025004 (2015)
35. Krachkov P A, Lee R N, Milstein A I *Phys. Usp.* **59** 619 (2016); *Usp. Fiz. Nauk* **186** 689 (2016)
36. Krachkov P A, Milstein A I *Phys. Rev. A* **93** 062120 (2016)
37. Krachkov P A, Milstein A I *JETP* **126** 326 (2018); *Zh. Eksp. Teor. Fiz.* **154** 394 (2018)
38. Krachkov P A, Milstein A I *Phys. Lett. B* **771** 5 (2017)
39. Krachkov P A, Milstein A I *Nucl. Phys. A* **971** 71 (2018)
40. Gevorkyan S R et al. *Phys. Rev. A* **58** 4556 (1998)
41. Lee R N, Milstein A I, Strakhovenko V M, Schwarz O Ya *JETP* **100** 1 (2005); *Zh. Eksp. Teor. Fiz.* **127** 5 (2005)
42. Krachkov P A, Milstein A I *Phys. Rev. A* **91** 032106 (2015)
43. Krachkov P A, Lee R N, Milstein A I *Phys. Rev. A* **90** 062112 (2014)
44. Baur G, Hencken K, Trautmann D *Phys. Rep.* **453** 1 (2007)
45. Baltz A J et al. *Phys. Rep.* **458** 1 (2008)
46. Hencken K, Kuraev E A, Serbo V G *Phys. Rev. C* **75** 034903 (2007)
47. Ivanov D, Melnikov K *Phys. Rev. D* **57** 4025 (1998)
48. Jentschura U D, Serbo V G *Eur. Phys. J. C* **64** 309 (2009)
49. Downie E J, Lee R N, Milstein A I, Ron G *Phys. Lett. B* **728** 645 (2014)
50. Lee R N, Milstein A I *JETP* **109** 968 (2009); *Zh. Eksp. Teor. Fiz.* **136** 1121 (2009)